Bull. Spec. Astrophys. Obs., 2002, 54, 89-122

Experimental studies of the beam pattern of RATAN-600

E.K. Majorova, S.A. Trushkin

Special Astrophysical Observatory of the Russian AS, Nizhnij Arkhyz 369167, Russia

Received September 6, 2002; accepted September 23, 2002.

Abstract.
Results are presented of investigation of the beam pattern (BP) of the RATAN-600 radio telescope observing the bright discrete sources. The measurements were carried out in the range from 1.4 to 50 cm wavelength at the elevations of sources from 10 to 90 degrees and, for the first time, in a sufficiently large solid angle. The main beam of the BP was measured to a level of 0.5 – 2 % of the maximum. A comparison was made of calculated and experimental data in different horizontal cross-sections of BP. It is shown that the new computation of the BP, which takes account of the diffraction effects, and the finite size of the RATAN-600 main mirror ring have a better fit to the data of measurements than the early calculations. It is shown how the structure of the BP will change at distant cross-sections with the variations of amplitude and distribution of the errors in settings of the main mirror reflecting elements. The aberration curves were measured that describe the fall-down of signal in observations with transverse shifts of the horn from the antenna focus. The computed curves were in good agreement with the measurements. A comparison was made of the drift scans of the Moon with the convolutions of the two-dimensional computed BP with the uniform disk of angular dimensions of the Moon, the root-mean-square error of setting the main mirror panels is estimated. It is equal to 0.55 ± 0.05 mm. Taking into account a good agreement between the theoretical electrodynamic calculation of the BP and the measurement data, it can be recommended for modeling astrophysical experiments at RATAN-600 and for inclusion of this refined calculation of the BP in the data-processing procedures of current observations.

Key words: telescope: radio — antenna beam — beam pattern: calibration

1. Introduction

Measurements of fluxes and radio brightness distributions of extended cosmic sources, processing of data of deep surveys and investigation of anisotropy of the relic background demand true knowledge of the BP of the radio telescope in a large solid angle and in the total working wavelength range. The telescope RATAN-600 is a variable profile antenna, the shape and the width of its BP vary considerably depending on the elevation of the observed source, therefore it is impossible to measure the BP for all possible configurations of the antenna. It seems more logical to use the calculated BPs having checked their consistency to the BP measured with the radio astronomy technique of BP investigation from observations of bright point cosmic sources (Kus'min and Solomonovich, 1964).

This method was earlier used by Temirova (1983, 1985) to measure horizontal and vertical cross-sections of the BP at wavelengths 3.9 and 8.2 cm. The experimental relationships between the halfwidth of the BP and the elevation of the observed source, that she constructed, were in good agreement with the computed ones except for low elevations. After a more precise method of computation of the BP (Majorova, 2002), which allowed for the diffraction effects in the space between the main and secondary mirrors, had been developed, we decided to come back to this question and test the BP calculation in a wider solid angle and in the range 1.4–49 cm wavelength both in the mode of the focused antenna and in the presence of aberrations. It should be noted that the antenna has changed considerably since the 1980s. The vertical size of the main mirror panels has been increased from 7.4 m to 11.4 m. The setting of the antenna to the source is performed now with the aid of an automated control system (ACS). New high sensitivity radiometers have appeared. The working wavelength range has been increased. We believed that measurements of the BP could give new information about the state of the antenna and its characteristics. To investigate the weak scattered background around the main lobe of the telescope BP, it was supposed to carry out observations of the Moon.

2. Measurements

The BP of the North sector of the RATAN-600 radio telescope was measured in three sets of observations (2001 February-March, 2001 October, 2002 April). Sources were observed in the upper culmination in the mode of transit of a source across the immovable BP of the telescope. The flux densities of the sources were above 3 Jy. The high sensitivity radiometric complex of the feed-cabin No. 1 was used for the measurements. The sensitivity of its radiometers is 3 mK at the wavelengths 2.7 and 3.9 cm, 2.5 mK at 7.6 cm, 8 mK at 13 cm, 15 and 20 mK at the wavelengths 31 and 49 cm, respectively. Thus, with the effective area of about $1000\,\mathrm{m}^2$ a high signal-to-noise ratio was realized in one observation even in the cross-sections far from the central one. In the process of observations the curves of point source transit across different horizontal (azimuthal) cross-sections of the BP were registered and their primary processing was performed. Further processing of drift scans records consisted in their reduction to the antenna temperatures, background subtraction and normalization.

Because the angular dimensions of the observed sources are much smaller than the BP width, the antenna response at the output of the radiometer coincides with an accuracy to the constant factor with the BP of the radio telescope (F) in a given cross-section. Transits of sources with an elevation H were observed across the horizontal cross-section of the BP which differed in elevation from the central horizontal cross-section by ΔH.

In order to cover the whole range of elevations, the following sources: PKS 0521–36 ($H = 9.8°$), PKS 1830−21 ($H = 25.1°$), 3C 161 (0624−05) ($H = 40.3°$), 3C 273 (1226+02) ($H = 48.2°$), 3C 454.3 (2251+158) ($H = 62.3°$), 3C 123 (0433+29) ($H = 75.8°$), TXT2005+403 ($H = 86°$), 3C84 (0316+41) ($H = 87.7°$) were chosen.

¿From the results of observations the relationships $F_{max}(\Delta H)$ were plotted, where F_{max} was the maximum value of the BP in the cross-section $H + \Delta H$ normalized to the BP maximum in the central section $\Delta H = 0$. Since the receiving horns are arranged along the focal line of the secondary mirror, the cross-sections of the BP were registered simultaneously at all wavelengths during one observation. Depending on the location of the receiving horn with respect to the focus of the antenna system, the BPs of both the focused antenna and the antenna with aberrations were measured. The observations were defined by the transverse displacement (Δ) of the receiving horn from the antenna focus.

3. Results of measurements of the BP

In the observations of February-March, 2001 the measurements of the BP were made at the waves λ2.7, 3.9, 7.6, 13 and 31 cm and at the elevations $H = 25.1°$ (PKS 1830−21) and 86° (TXT2005+403). The receiving horn at 7.6 cm (Δ=0) was placed at the antenna focus, the horn at the wavelength 2.7 cm was shifted from the focus by 9.4λ, at the wavelength 3.9 cm by 7.8λ, at 13 and 31 cm by 4.6λ and 1.9λ, respectively. The squares in Fig.1 show the data of measurement of F_{max}, the solid lines are for the relations $F_{max}(\Delta H)$ computed with the allowance for the diffraction effects in the Fresnel zone and finite width of the main mirror ring (Majorova, 2002), the dotted lines represent the relations $F_{max}(\Delta H)$ calculated by Korzhavin's (1979) programs (the formulae for the calculation were derived by Esepkina et al. (1979)). The relations $F_{max}(\Delta H)$ for the focused antenna are the vertical BPs of the radio telescope since the maxima of the drift scans lie in the same vertical plane. In the presence of lateral aberrations the maxima of the drift scans are in different vertical planes.

It can be seen in Fig. 1 that the experimental points obtained for the elevations $H = 25°$ and 86° are in good agreement with the curves $F_{max}(\Delta H)$ computed by the program of Majorova (2002). For $H = 25°$, the curves computed by Korzhavin's programs show discrepancies with the experimental points, the discrepancies being larger with growing shift of the receiving horn from the antenna focus. For high elevations of sources ($H = 86°$) the computations by the program of Korzhavin show a good agreement with the experiment and are practically coincident with the results of calculation by the new program.

Figs. 2–7 present the drift scans of the sources PKS 1830–21 and TXT 2005+403 along the horizontal cross-sections of the BP (thin line) and the calculated cross-sections of the BP (bold lines) with allowance made for the diffraction effects. The drift scans are normalized to the signal maximum in the central cross-section. In these figures and the plots presented below, where the drift scans of the sources are shown, the abscissa is the time scale (right ascension). Seconds of time (sec) are converted in the ordinary manner to angular seconds ($\times 15\cos\delta$), the elevations of the source are $H = 90 - \phi + \delta + Ref$, where δ is the visible declination of the source, ϕ is the latitude of RATAN-600, Ref is the radio refraction.

At short wavelengths ($\lambda \leq 7.6$ cm) the cross-sections of the BP were measured up to the levels of 0.02–0.05 from $F_{max}(0)$. A good agreement between the experimental and the computed curves was obtained. Unfortunately, due to the shortage of observational time, the BPs in this set were measured only at

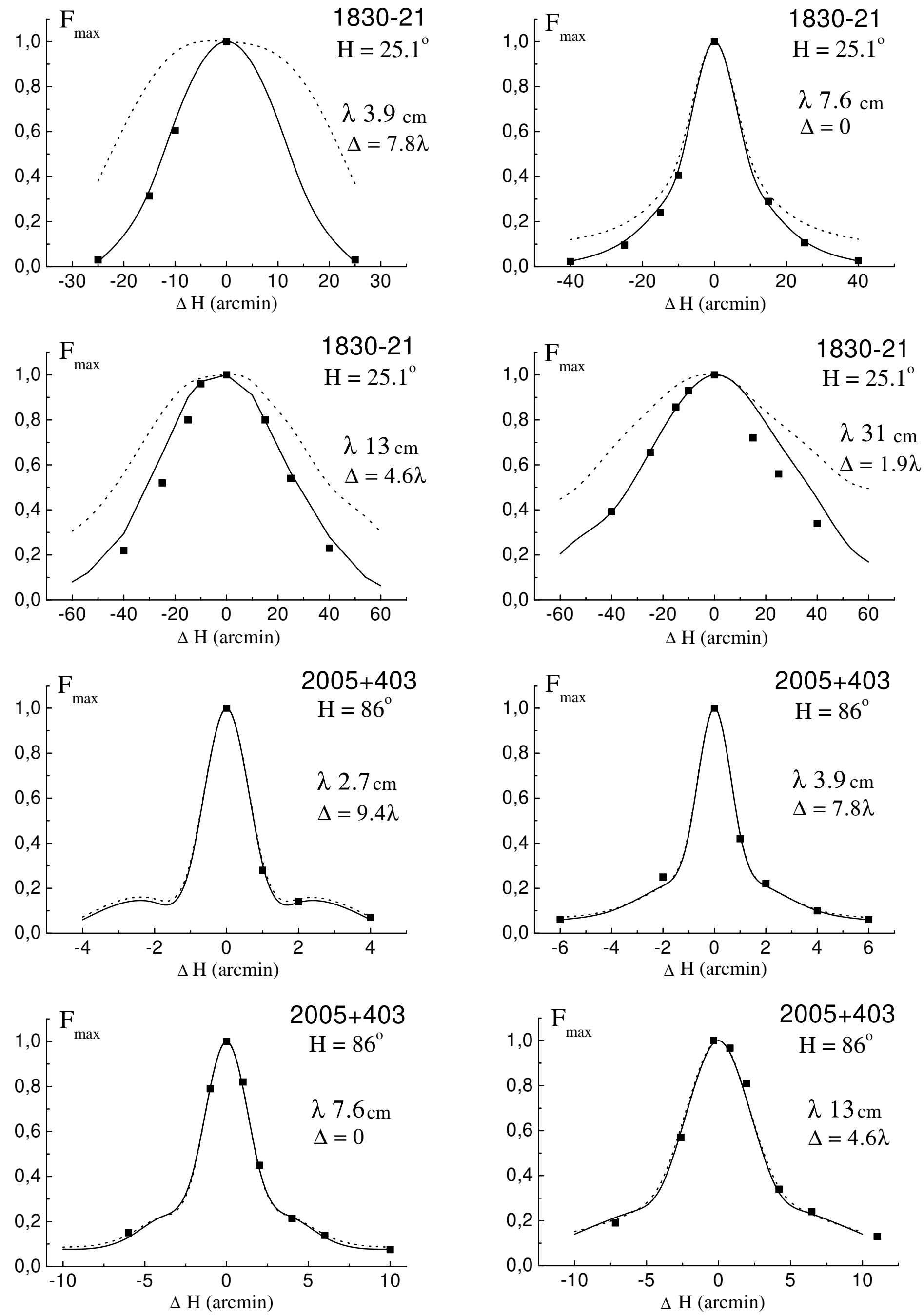

Figure 1: *The relations between the maximum value of the BP F_{max} in different horizontal cross-sections and the shift value of the section (ΔH) in elevation with respect to the central cross-section. The squares show the data of measurements made in 2001 February-March, the solid lines are the computations of Majorova (2002), the dotted lines show the computations by the program of Korzhavin (1979). All the values of F_{max} are normalized to the maximum of the BP in the central cross-section.*

two elevations, experimental relations $F_{max}(\Delta H)$ at $\lambda 13, 31$ cm ($H = 25°$) were obtained only to the levels 0.2–0.3 $F_{max}(0)$ and had certain discrepancies with the computed curves which were probably caused by the small number of observations.

In the 2001 October observations the BP was measured at the wavelengths $\lambda 3.9 - 49$ cm in the wider solid angles. When observing the sources PKS 0521–36 ($H = 9.8°$), 3C 161 (0624–05) ($H = 40.3°$), 3C 454.3 (2251+158) ($H = 62.3°$), 3C 123 (0433+29) ($H = 75.8°$), 3C84 (0316+41) ($H = 87.7°$) the horns with the same phase center at the wavelengths $\lambda 13$,

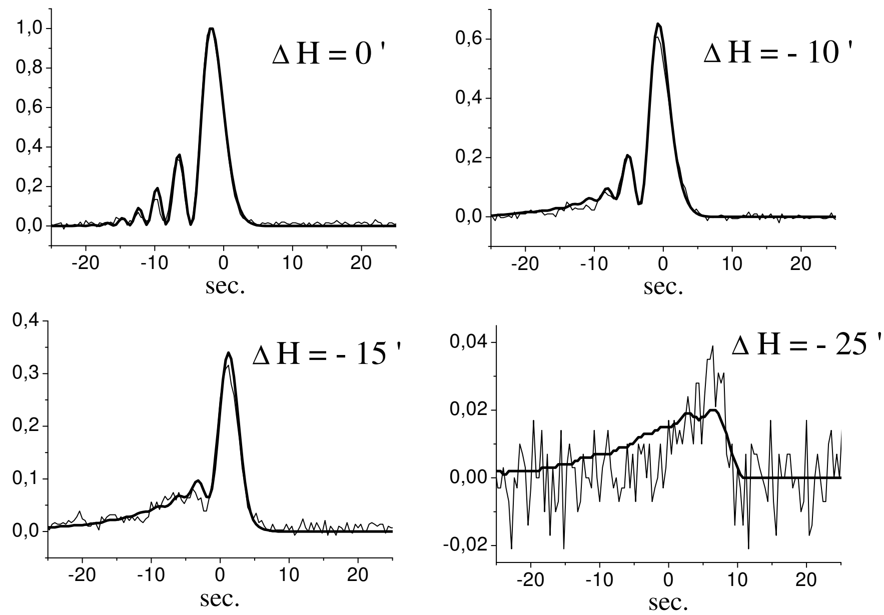

Figure 2: *The drift scans of the point source PKS 1830–21 (H=25°08′) at the wavelength λ3.9 cm across the horizontal cross-section of the BP (thin lines) and the computed horizontal cross-sections of the BP corresponding to them (bold lines). The observations were carried out in February-March, 2001. The shift of the horn is $\Delta = 7.8\lambda$.*

31 and 49 cm were placed at the antenna focus, in the observations of the sources PKS 1830–21 ($H = 25.1°$) and 3C 273 (1226+02) ($H = 48.2°$) the horn at λ7.6 cm was located at the antenna focus. Observations at the wavelengths λ 7.6, 13, 31 and 49 cm were carried out in the single-horn mode, at the wavelength λ3.9 cm — in the double-horn beam-switching mode.

The results of F_{max} measurements are shown by squares in Figs. 8–9. The relations $F_{max}(\Delta H)$ calculated with allowance for the diffraction effects in the Fresnel zone (solid lines) are also shown in these figures. As one can see from the figures, actually in the whole examined range of elevations and wavelengths the experimental points fit well enough to the computed curves. However, a detailed examination of the curves shows that for the majority of elevations the experimental relations are shifted with respect to the computed ones to the region of negative ΔH (by $1' \div 1.5'$). More clearly this effect manifests itself when comparing the experimental drift scans of sources across different cross-sections of the BP with the corresponding computed cross-sections of the BP (Figs. 10–19). For the sake of convenience of comparison, the experimental and computed curves are normalized to the maximum of the BP in the central cross-section.

The drift scans of point sources through different cross-sections of the BP are shown in Figs. 10–19 by the thin lines), the cross-sections calculated by the program of Majorova (2002) are represented by the bold lines. The elevations of the sources are $H = 9.8°$, 40.3°, 62.7°, 87.7°. The drift scans were registered in the cross-sections symmetrical about the central section of the BP, at the waves λ 31, 13, 7.6, 3.9 cm at different shifts of the receiving horn from the focus. From a comparison of the experimental and computed curves it is seen that in a first approximation their shapes coincide well. There are cross-sections where the coincidence of the experimental and computed curves is satisfied within $2 - 3\sigma$ above the system noises.

However, there are cross-sections where there is a good deal of discrepancy between the experimental and calculated curves. There exists a stable rule: for the cross-sections with positive ΔH, the maximum of the experimental curves $F^E{}_{max}$ is less or coincides with the values of the maxima of the computed curves $F^R{}_{max}$; for the cross-sections with negative ΔH an opposite picture is observed: $F^E{}_{max} \geq F^R{}_{max}$. This asymmetry of the BP was not observed in 2001 February-March, at least, at short wavelengths. Besides, at high angles ($H \geq 62°$) and wavelengths $\lambda \leq 7.6$ cm a change in the structure of the BP took place in distant cross-sections. The drift scans at the wave λ3.9 cm in the cross-sections $\Delta H = \pm 4' \div \pm 10'$ have got a small-scale structure. At the wave λ7.6 cm ($H = 87.7°$) the most essen-

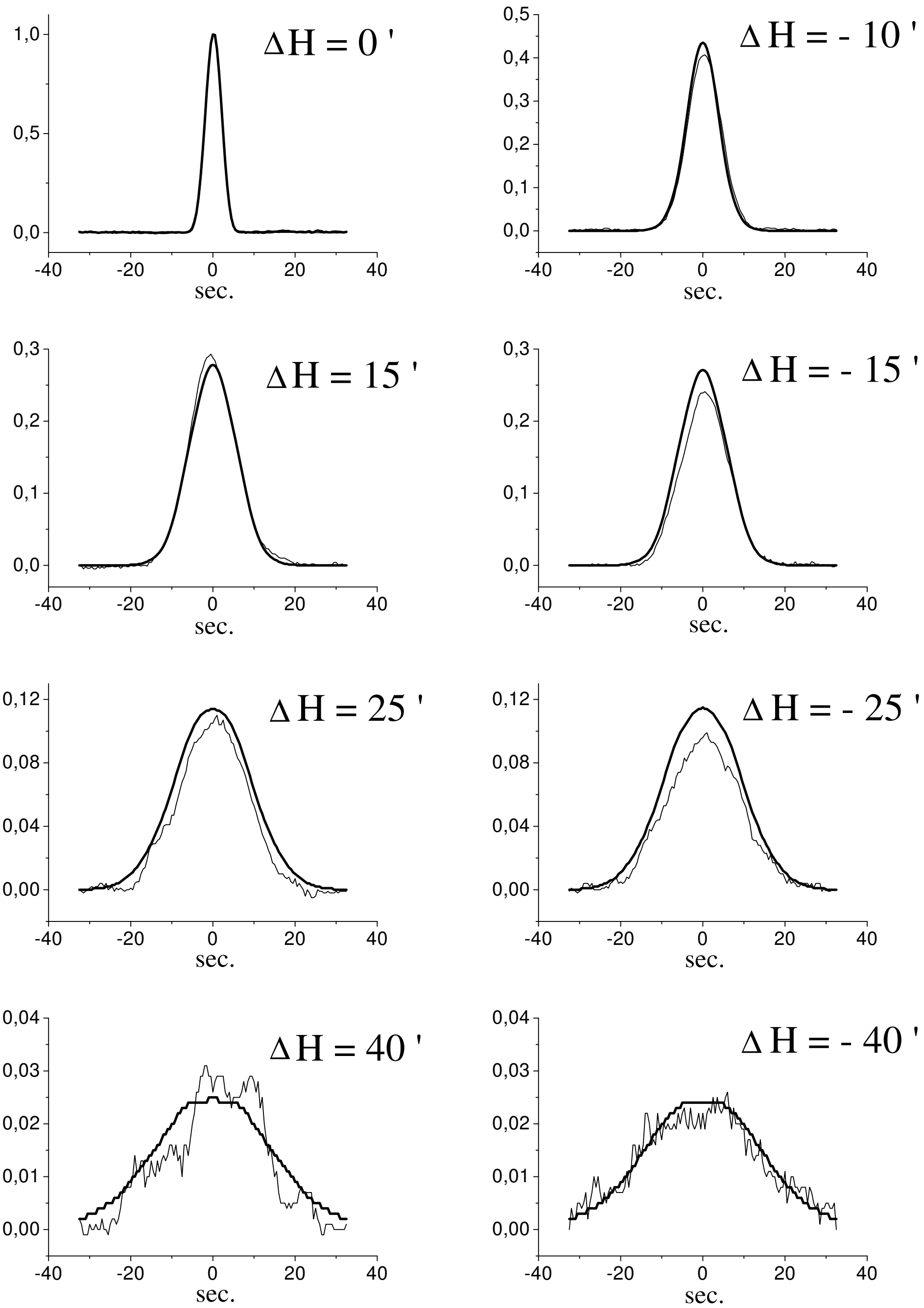

Figure 3: *The drift scans of the point source PKS 1830–21 (H=25°08′) at the wavelength λ7.6 cm across the horizontal cross-section of the BP (thin lines) and the computed horizontal cross-sections of the BP corresponding to them (bold lines). The observations were carried out in February-March, 2001. The shift of the horn is $\Delta = 0$.*

tial differences of the BP structure as compared with the calculated BP manifested themselves in the cross-sections $\Delta H = \pm 10,\ \pm 20'$. In still more distant cross-sections the drift scans are much closer to the computed ones, if the noise component is smoothed. We will discuss this below.

Using the observational data of this run, experimental two-dimensional BPs at the waves λ13 and 7.6 cm were constructed. In Fig. 20 these BPs are presented as isophotes 0.01, 0.018, 0.032, 0.056, 0.1, 0.18, 0.32, 0.56. The BPs are normalized to the maximum in the central cross-section. When constructing experimental two-dimensional BPs, the drift scans of sources across equally spaced cross-sections were

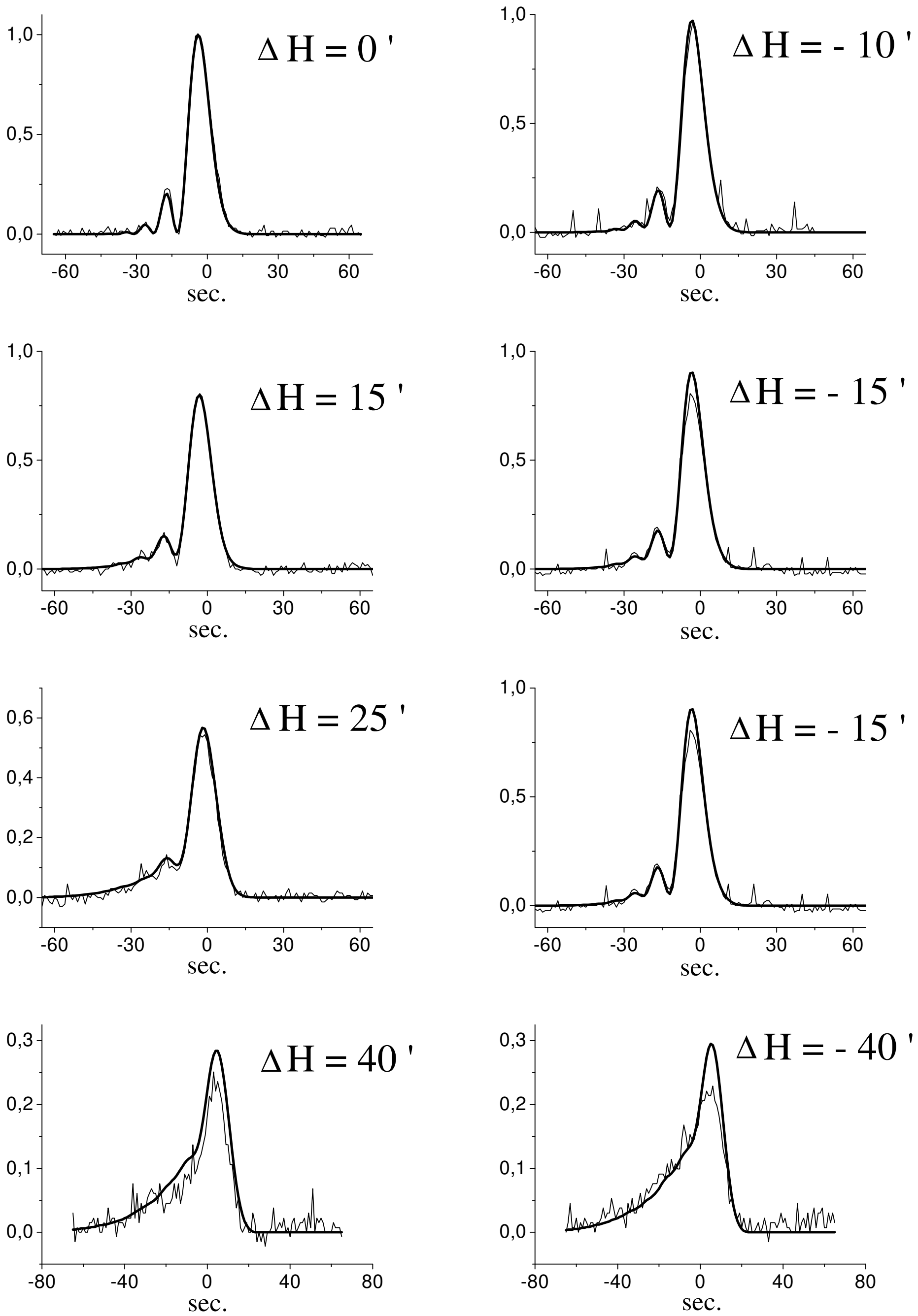

Figure 4: *The drift scans of the point source PKS 1830–21 (H=25°08′) at the wavelength λ13 cm across the horizontal cross-section of the BP (thin lines) and the computed horizontal cross-sections of the BP corresponding to them (bold lines). The observations were carried out in February-March, 2001. The shift of the horn is* $\Delta = 4.6\lambda$.

used.

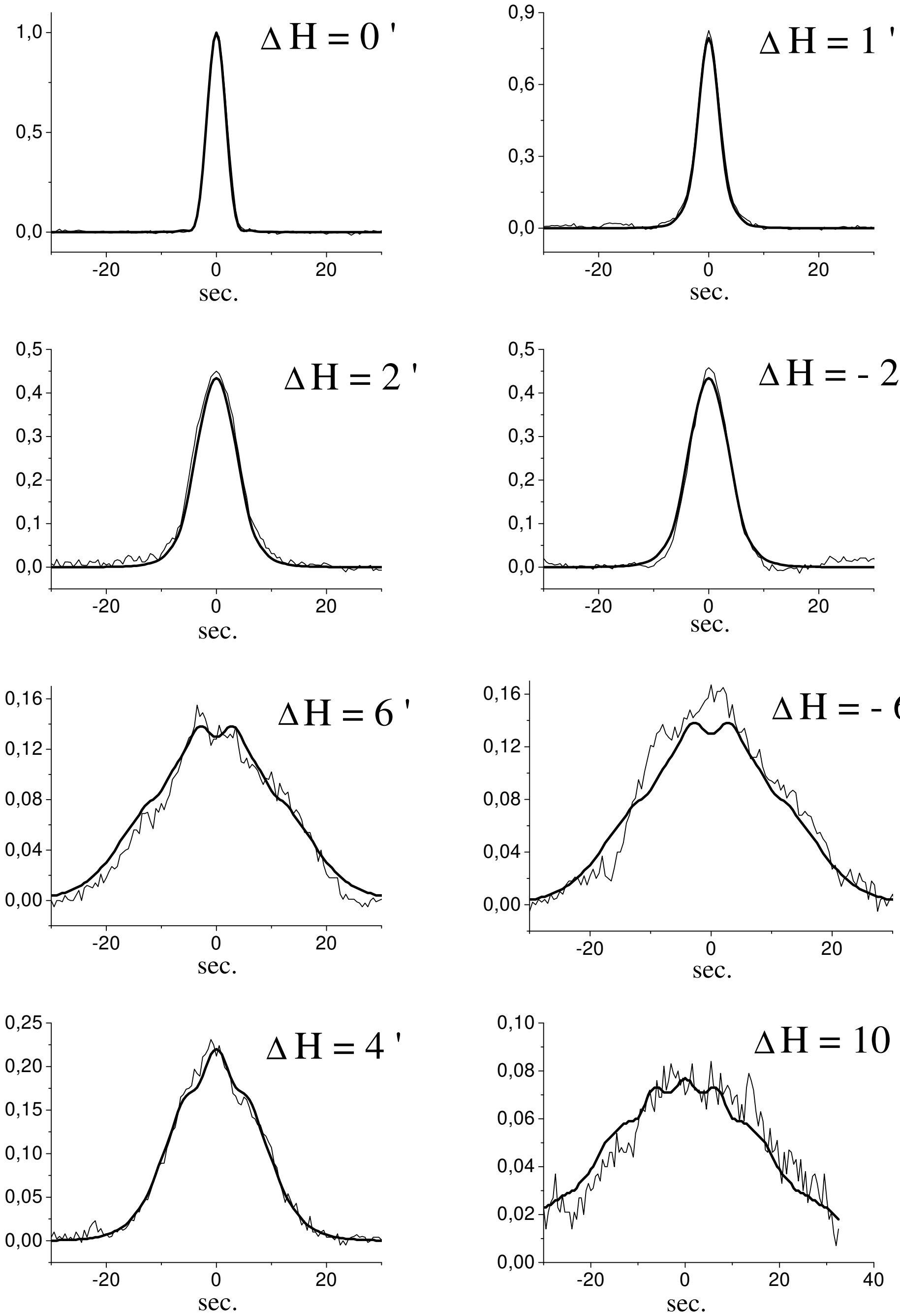

Figure 5: *The drift scans of the point source TXT2005+403 (H=86°40′) at the wavelength λ7.6 cm across the horizontal cross-section of the BP (thin lines) and the computed horizontal cross-sections of the BP corresponding to them (bold lines). The observations were carried out in February-March, 2001. The shift of the horn is* $\Delta = 0$.

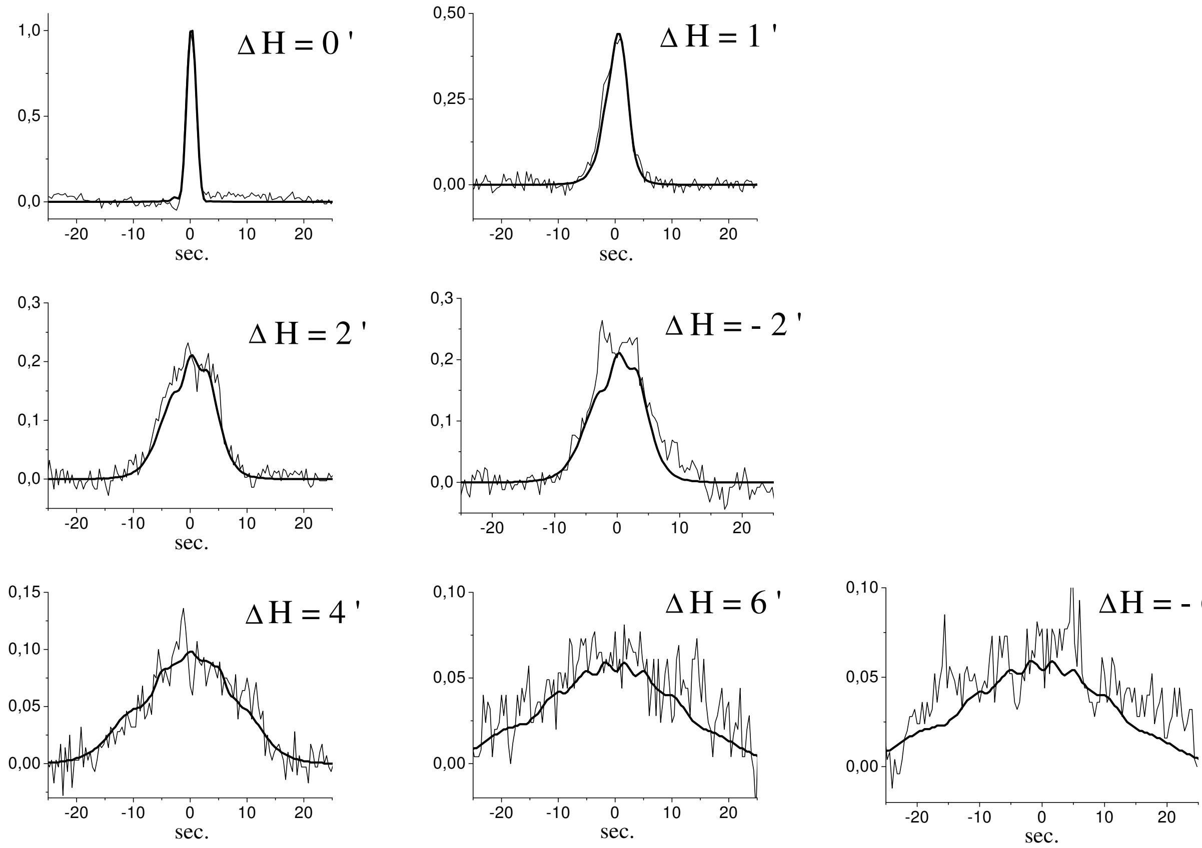

Figure 6: *The drift scans of the point source TXT2005+403 (H=86°40′) at the wavelength λ3.9 cm across the horizontal cross-section of the BP (thin lines) and the computed horizontal cross-sections of the BP corresponding to them (bold lines). The observations were carried out in February-March, 2001. The shift of the horn is* $\Delta = 7.8\lambda$.

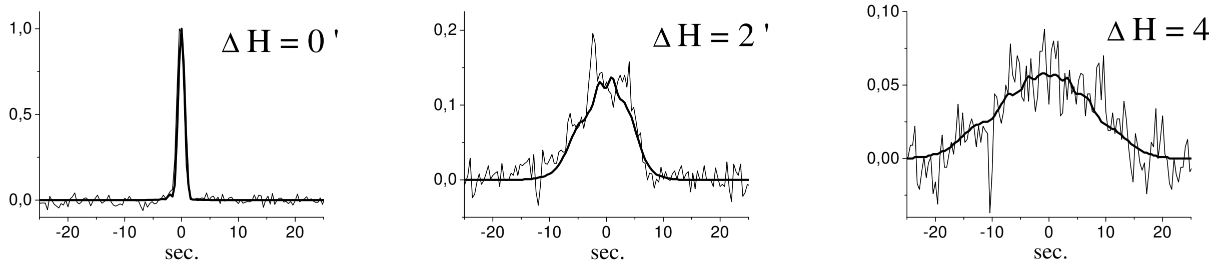

Figure 7: *The drift scans of the point source TXT2005+403 (H=86°40′) at the wavelength λ2.7 cm across the horizontal cross-section of the BP (thin lines) and the computed horizontal cross-sections of the BP corresponding to them (bold lines). The observations were carried out in February-March, 2001. The shift of the horn is* $\Delta = 5.8\lambda$.

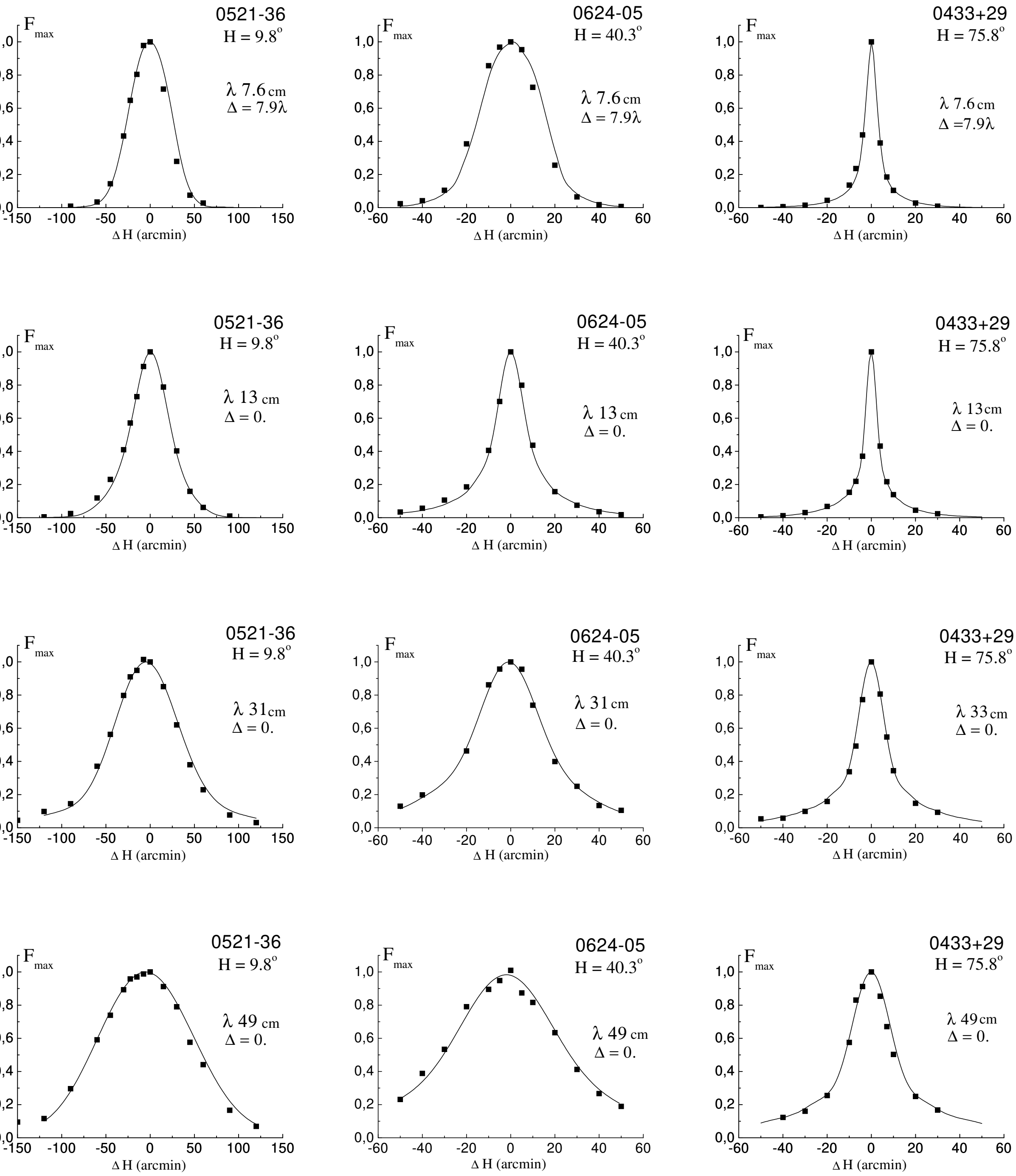

Figure 8: *The relationships $F_{max}(\Delta H)$. The squares show the data of measurements from the 2001 October set, the solid lines display the computation of the BP by the program of Majorova (2002).*

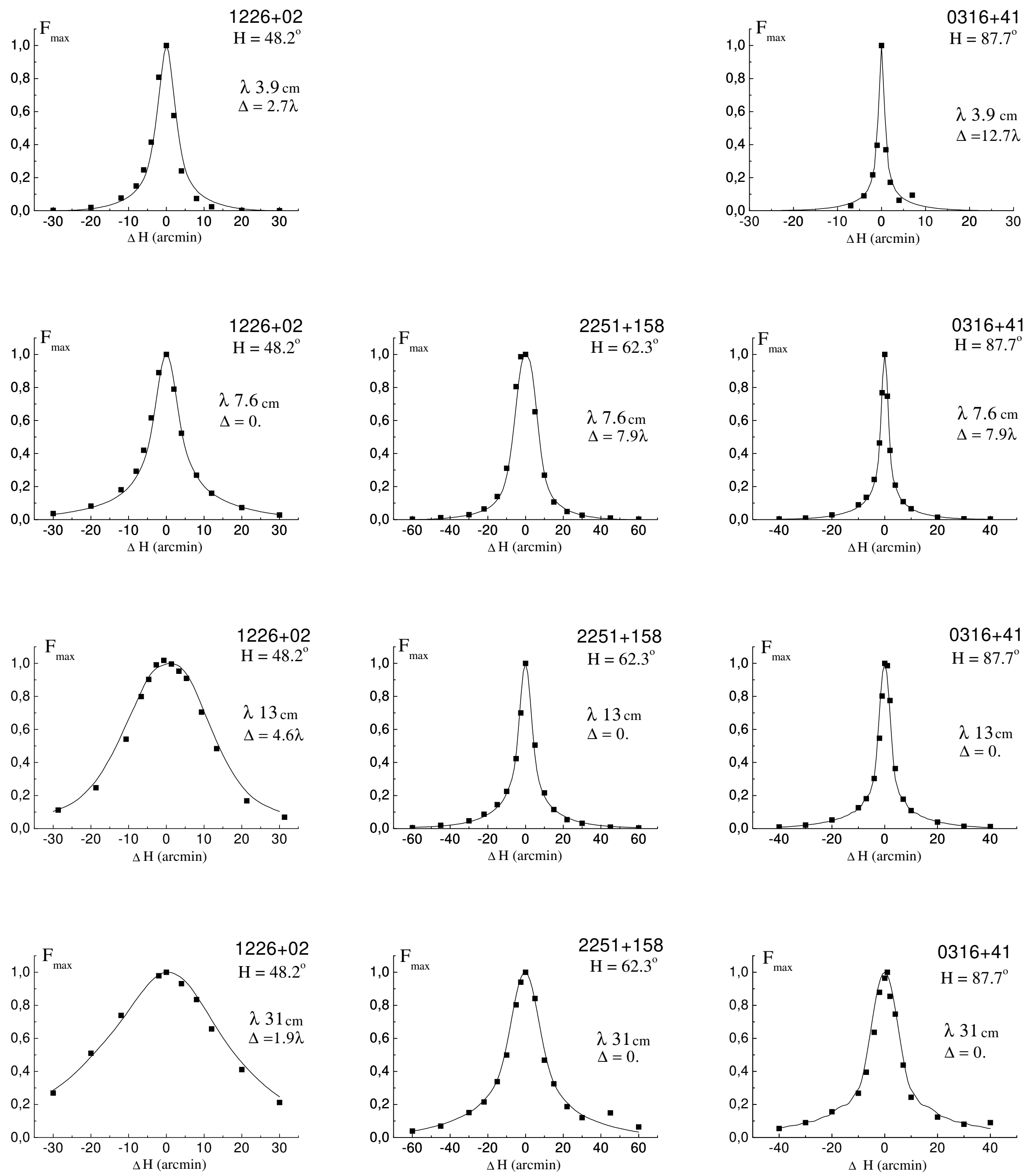

Figure 9: *The relationships $F_{max}(\Delta H)$. The squares show the data of measurements from the 2001 October set, the solid lines display the computation of the BP by the program of Majorova (2002).*

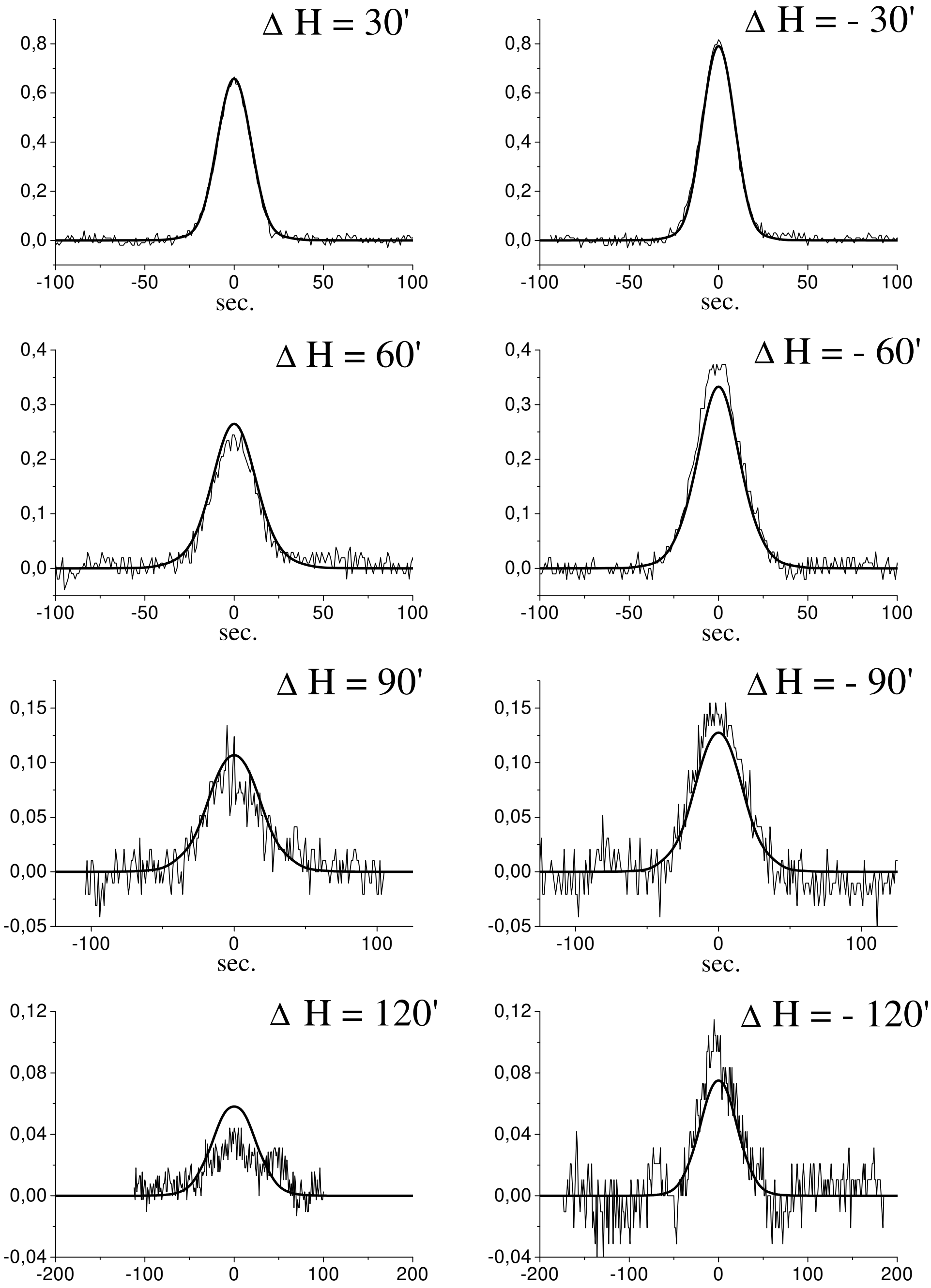

Figure 10: *The drift scans of the point source PKS 0521–36 (H=09°50′) at the wavelength λ31 cm across the horizontal cross-section of the BP (thin lines) and the computed horizontal cross-sections of the BP corresponding to them (bold lines). The observations were carried out in October, 2001. The shift of the horn is* $\Delta = 0$.

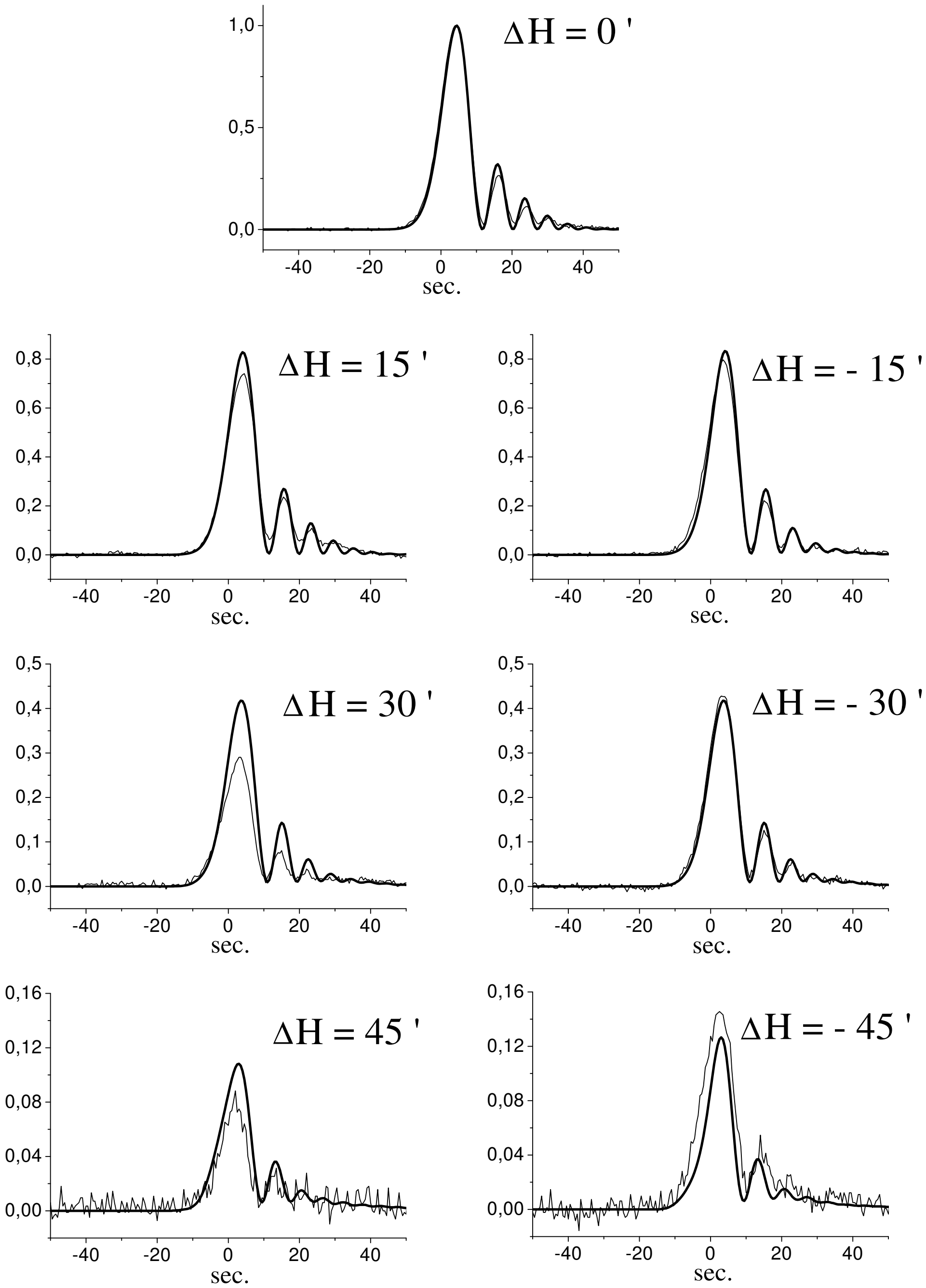

Figure 11: *The drift scans of the point source PKS 0521–36 (H=09°50′) at the wavelength λ7.6 cm across the horizontal cross-section of the BP (thin lines) and the computed horizontal cross-sections of the BP corresponding to them (bold lines). The observations were carried out in October, 2001. The shift of the horn is* $\Delta = 7.9\lambda$.

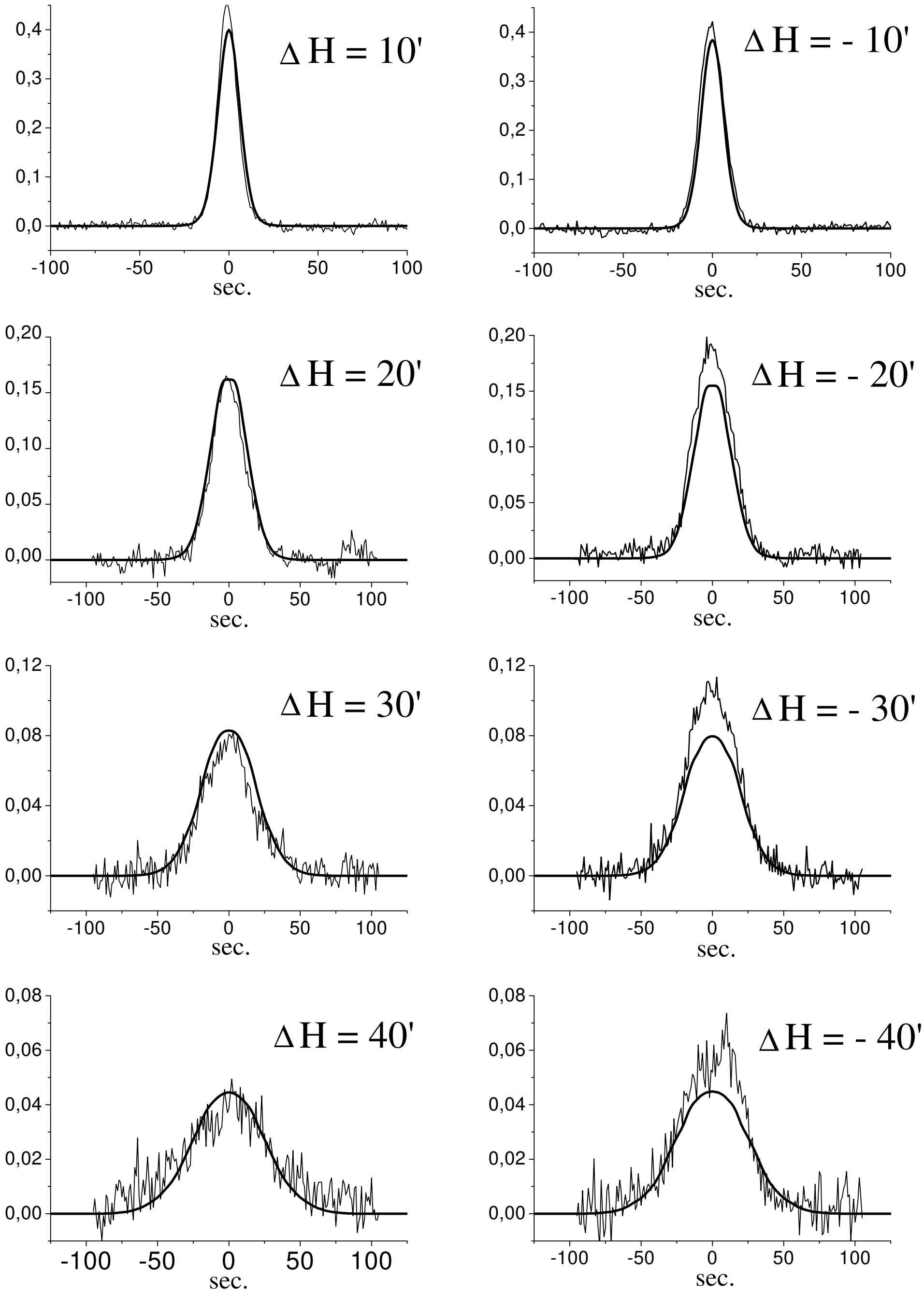

Figure 12: *The drift scans of the point source 3C 161 (0624-05) (H=40°18.5′) at the wavelength λ13 cm across the horizontal cross-section of the BP (thin lines) and the computed horizontal cross-sections of the BP corresponding to them (bold lines). The observations were carried out in October, 2001. The shift of the horn is* $\Delta = 0$.

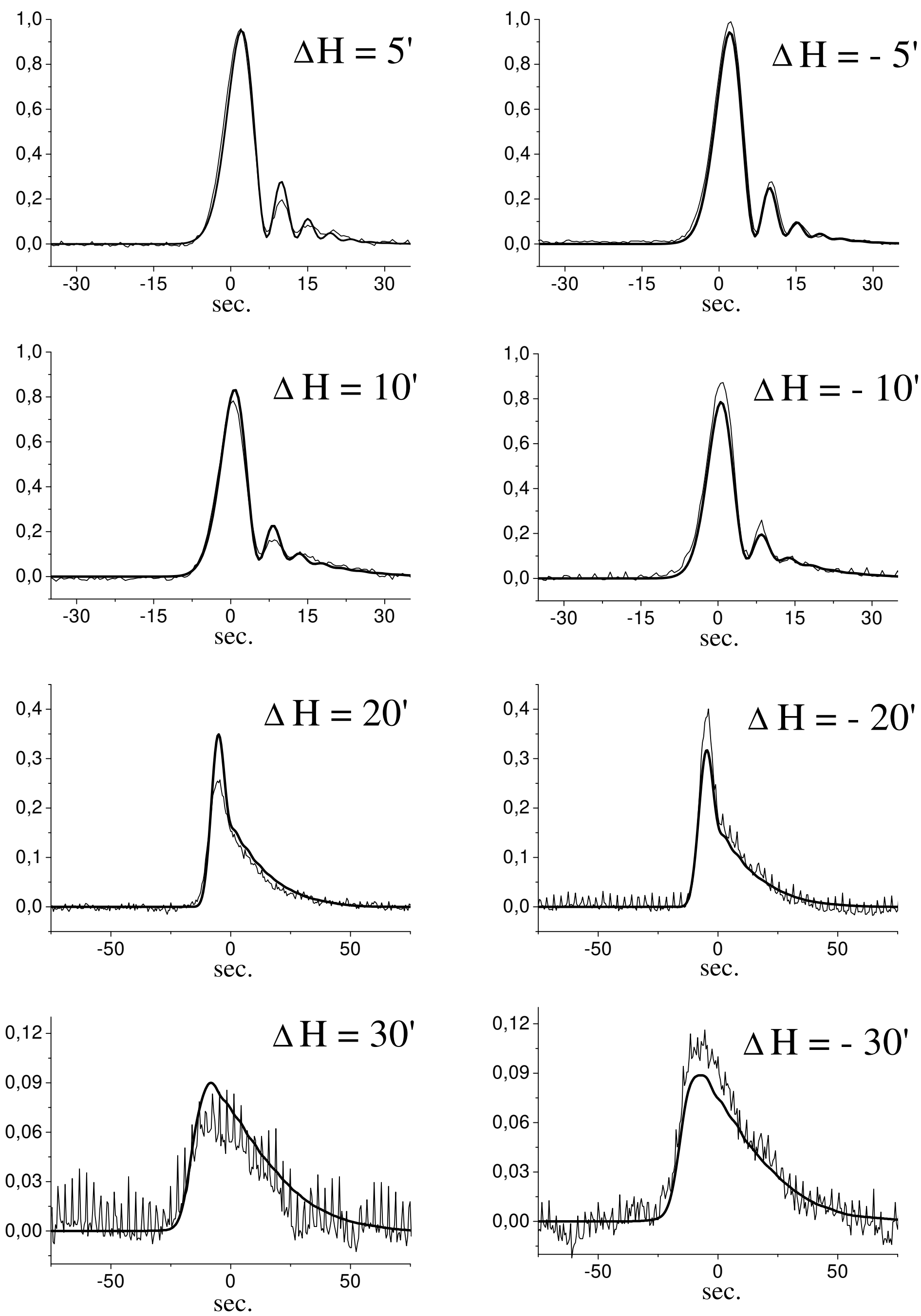

Figure 13: *The drift scans of the point source 3C 161 (0624-05) (H=40°18.5′) at the wavelength λ7.6 cm across the horizontal cross-section of the BP (thin lines) and the computed horizontal cross-sections of the BP corresponding to them (bold lines). The observations were carried out in October, 2001. The shift of the horn is* $\Delta = 7.9\lambda$.

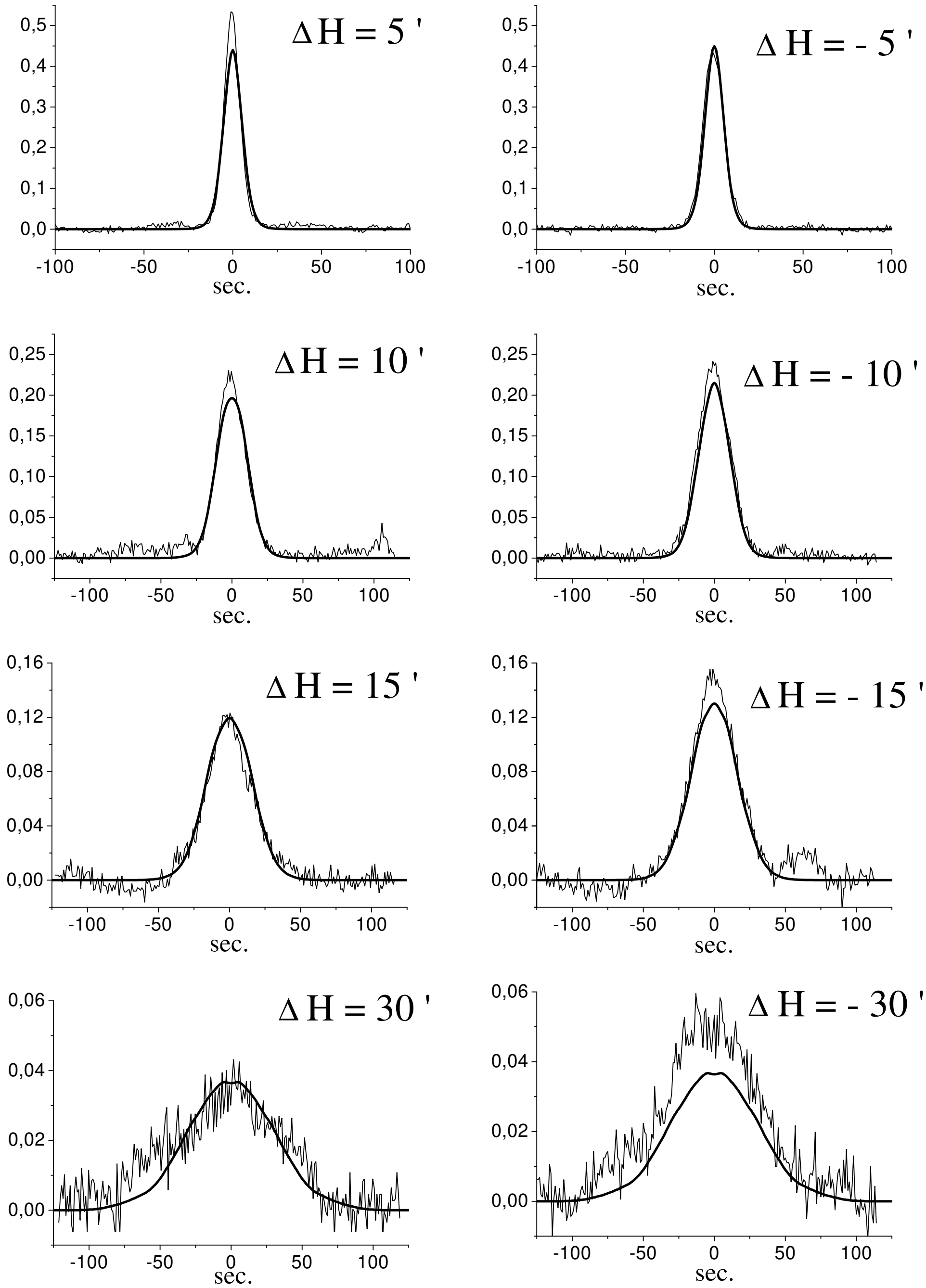

Figure 14: *The drift scans of the point source 3C454.3 (2251+158) (H=62°20′) at the wavelength λ13 cm across the horizontal cross-section of the BP (thin lines) and the computed horizontal cross-sections of the BP corresponding to them (bold lines). The observations were carried out in October, 2001. The shift of the horn is* $\Delta = 0$.

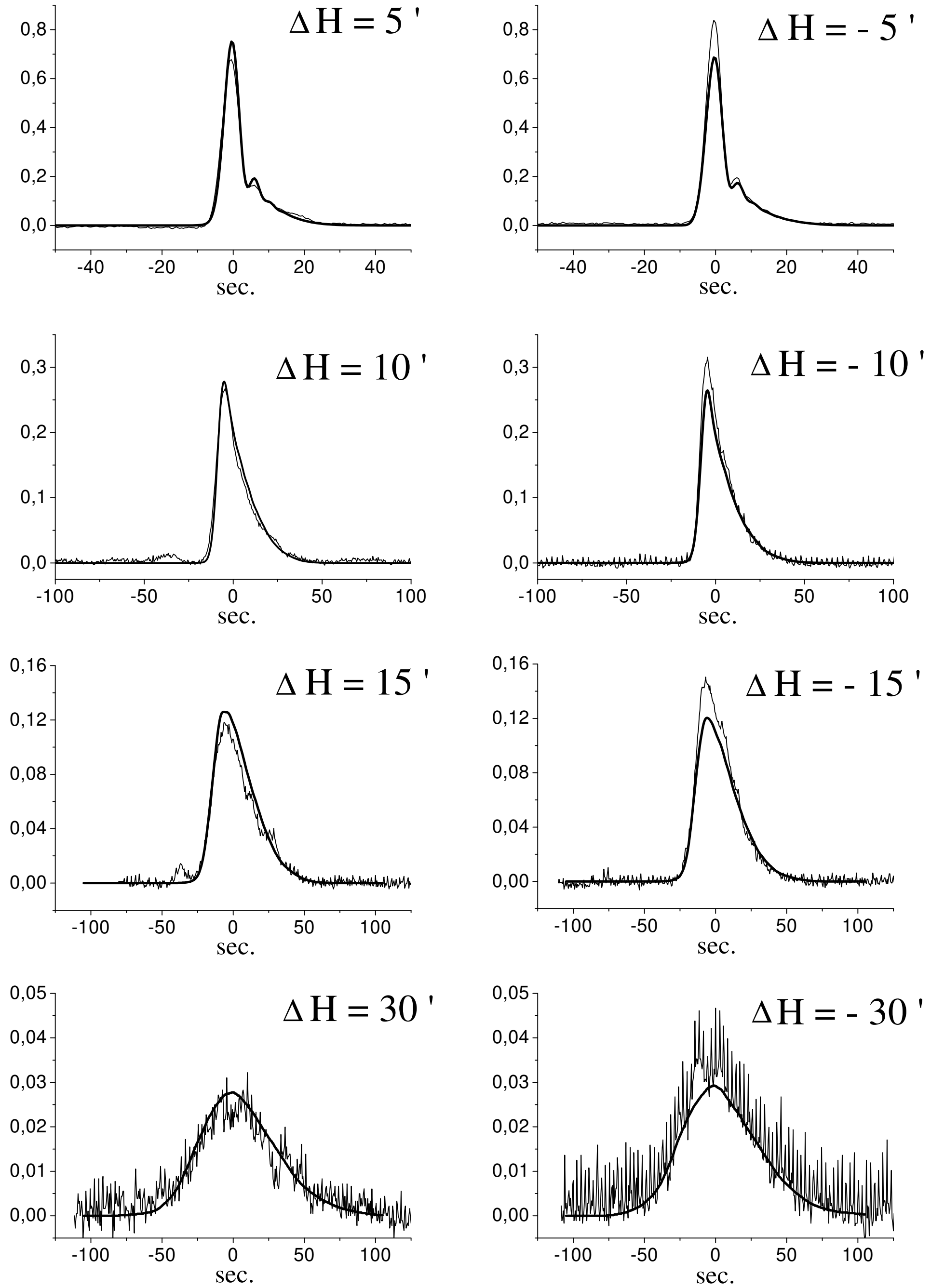

Figure 15: *The drift scans of the point source 3C454.3 (2251+158) (H=62°20′) at the wavelength λ7.6 cm across the horizontal cross-section of the BP (thin lines) and the computed horizontal cross-sections of the BP corresponding to them (bold lines). The observations were carried out in October, 2001. The shift of the horn is $\Delta = 7.9\lambda$.*

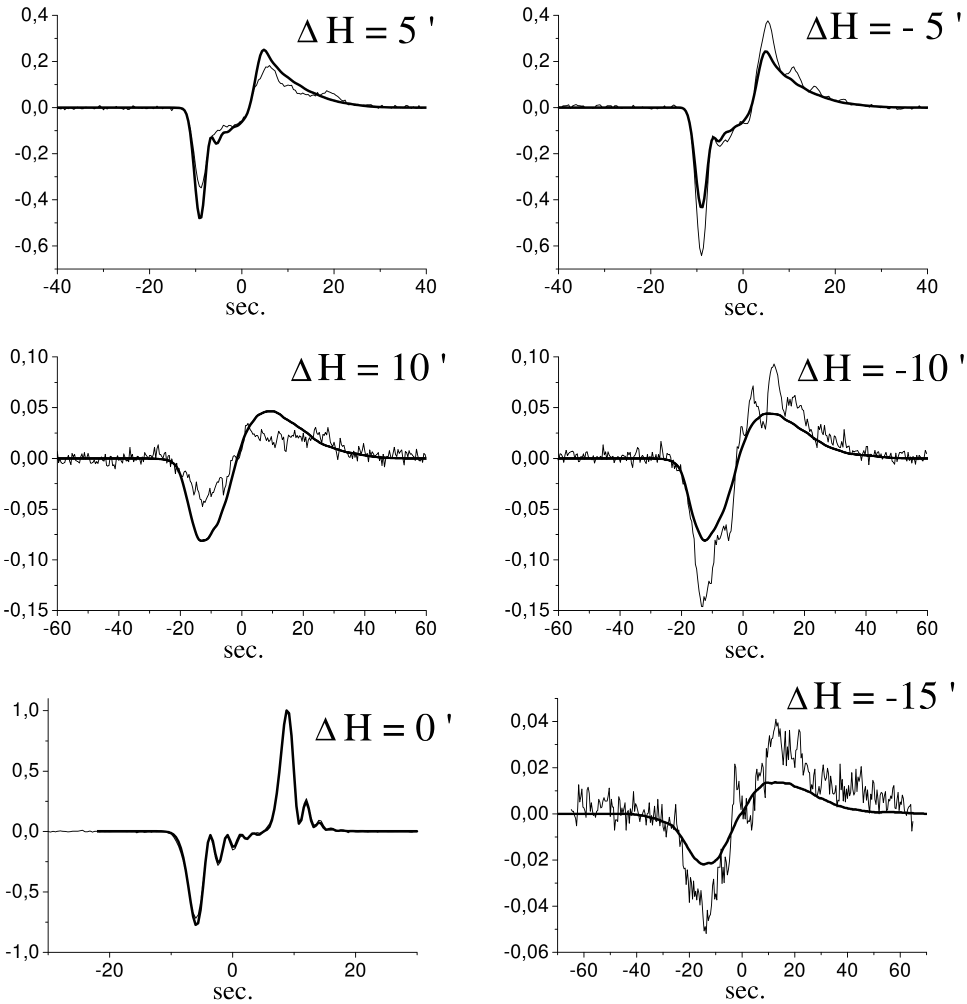

Figure 16: *The drift scans of the point source 3C454.3 (2251+158) (H=62°20′) at the wavelength λ3.9 cm across the horizontal cross-section of the BP (thin lines) and the computed horizontal cross-sections of the BP corresponding to them (bold lines). The observations were carried out in October, 2001. The shifts of the horns are* $\Delta = 12.7\lambda$ *and* 7.5λ.

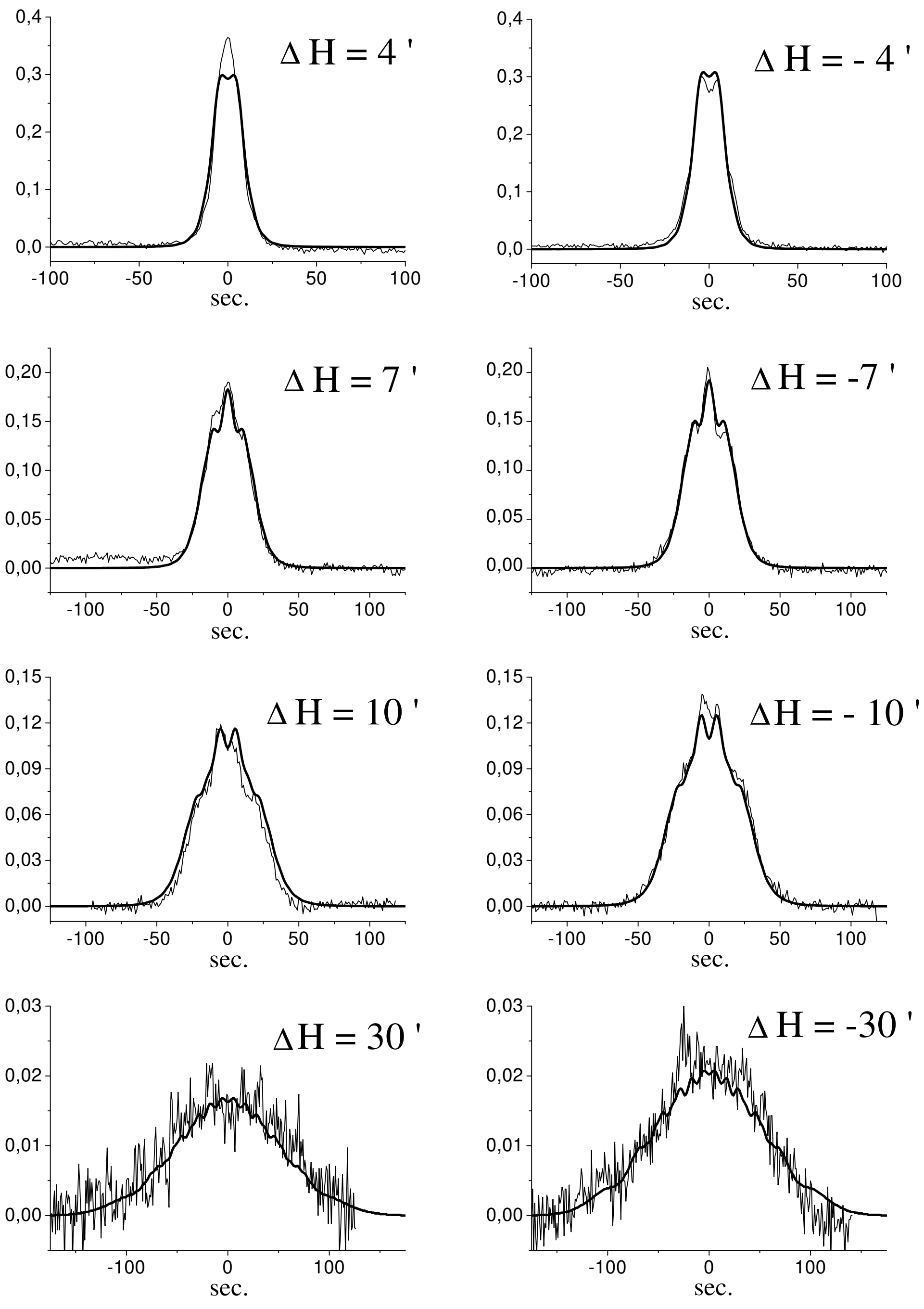

Figure 17: *The drift scans of the point source 3C84 (0316+41)(H=87°41′) at the wavelength* λ13 *cm across the horizontal cross-section of the BP (thin lines) and the computed horizontal cross-sections of the BP corresponding to them (bold lines). The observations were carried out in October, 2001. The shift of the horn is* $\Delta = 0$.

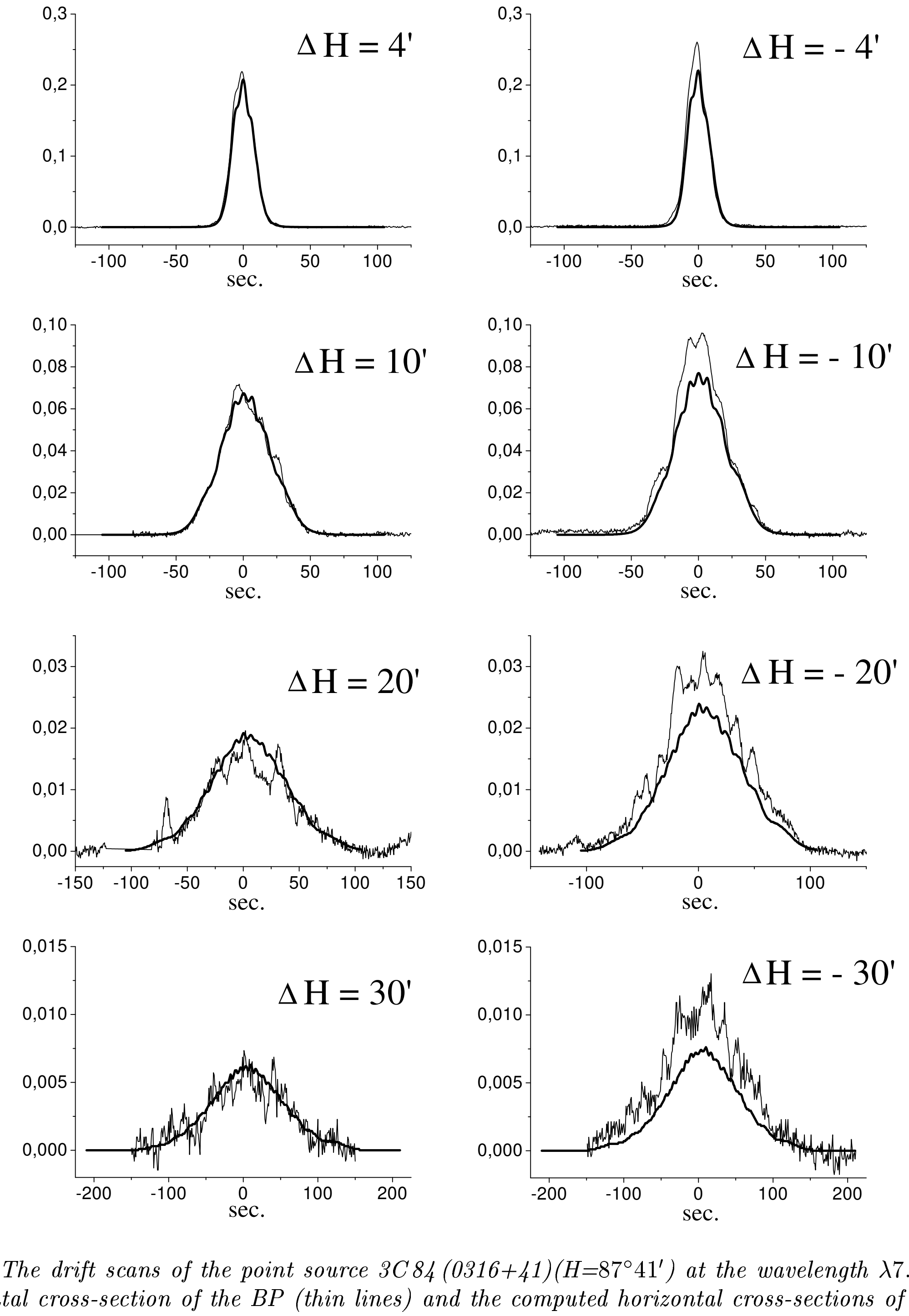

Figure 18: *The drift scans of the point source 3C 84 (0316+41)(H=87°41′) at the wavelength* λ7.6 *cm across the horizontal cross-section of the BP (thin lines) and the computed horizontal cross-sections of the BP corresponding to them (bold lines). The observations were carried out in October, 2001. The shift of the horn is* $\Delta = 7.9\lambda$.

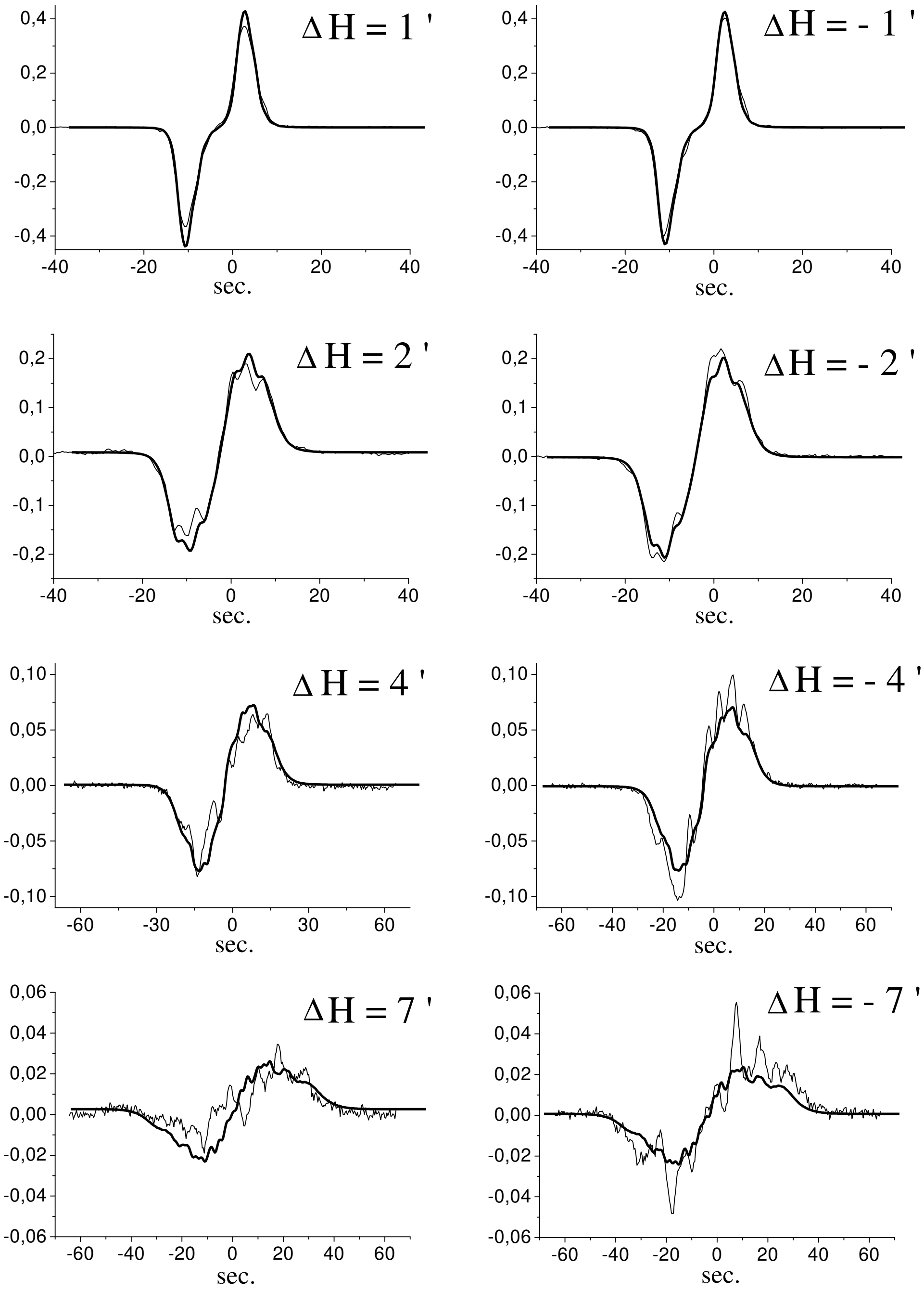

Figure 19: *The drift scans of the point source 3C 84 (0316+41)(H=87°41′) at the wavelength λ3.9 cm across the horizontal cross-section of the BP (thin lines) and the computed horizontal cross-sections of the BP corresponding to them (bold lines). The observations were carried out in October, 2001. The shifts of the horns are* $\Delta = 12.7\lambda$ *and* 7.5λ.

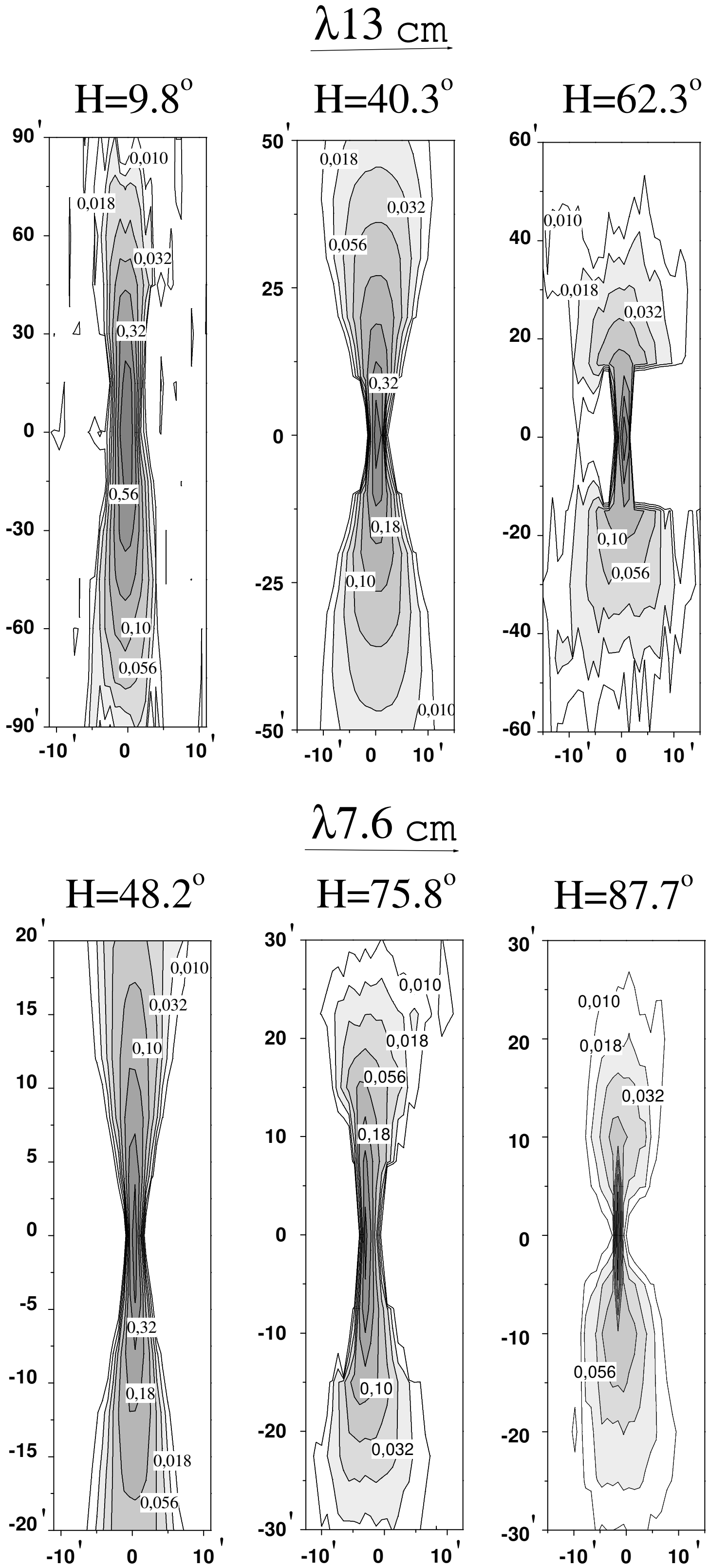

Figure 20: *The experimental two-dimensional BP of RATAN-600 at the waves λ7.6 and 13 cm plotted from the results of the 2001 October observations.*

In 2002 April repeat measurements of the BP were made with the North sector from the source 3 84(0316+41) ($H = 87.7°$) at the wavelength $\lambda 7.6$ cm. A month before the observations with this sector an auto-collimation adjustment was performed. Since from the moment of adjustment a comparatively short time had elapsed (for comparison: the 2001 February-March observations were conducted 4 months and the 2002 October observations were made 6 months after the antenna adjustment), it was supposed to measure the RATAN-600 BP with a high quality surface of the main mirror and compare the measurement results with those obtained in the previous cycle. The observations were repeated in the cross-sections $\Delta H = \pm 10', \pm 20', \pm 30'$. The drift scans corresponding to these cross-sections are shown in Figs. 21 and 22 by thin lines. The computed BP in these cross-sections are shown by bold lines. In addition the drift scans in the cross-sections $\Delta H = \pm 3', \pm 6', \pm 12', \pm 18', \pm 24'$ (Figs. 21 and 22) have been measured. One more source that fell within the BP of the radio telescope is seen in the records with negative ΔH at the left. For some cross-sections several records of drift scans were obtained. Fig. 23 presents three records of the cross-section $\Delta H = -20'$.

The drift scans measured in this run in the cross-sections $\Delta H = \pm 10', \pm 20', \pm 30'$ are significantly different from those obtained in the previous set and agree very well with the results of calculations. The rms of the difference of the records of the experimental and computed drift scans was no greater than $2 - 3\sigma$ of the noise level or 0.1–0.3 % of $F_{max}(0)$. The records of the difference between the drift scans measured on different days (Fig. 23) also had a dispersion of about two noise dispersions of the system. We did not foreknow that the shape of the drift scans measured at the cross-sections $\Delta H = \pm 12', \pm 18', \pm 24'$, recorded at the end of the set, are so strongly distorted. In these cross-sections the same small-scale structure was revealed which was seen in the cross-sections $\pm 20'$ in the previous observing run. We will investigate this point in the next chapter using additional information about the state of the antenna.

4. Discussion of the observational results

While discussing the technique of computation of the radio telescope BP, it should be emphasized that the formulae for the BP calculation were deduced under the assumption that the main and secondary mirrors of RATAN-600 are perfect smooth surfaces. In actual fact, the main mirror consists of separate reflecting elements (panels), which when moved in three coordinates (position angle, azimuth and radius) form a surface of a desired configuration. The affinity of the really formed surface with the ideal one is defined by the accuracy of adjustment and kinematic corrections to antenna elements settings, and also by the reliability of the mechanisms of the main mirror panels themselves and the ACS controlling their settings. The surface of the mirror may deteriorate because of changing of the real positions of elements between the current adjustments and failure of mechanisms. In order to take account of the effects these factors have on the BP of the radio telescope, firstly, one has to know exactly how the position of a panel has changed in each of the coordinates and, secondly, to allow in the calculations for these changes in the phase distributions of the field in the main mirror aperture.

To make possible taking into account the errors in setting of individual antenna elements the following changes were introduced in the program of calculation of the BP (Majorova, 2002). When integrating with respect to the angle ε (polar angle in the main mirror aperture), the number of points in the aperture was assumed to be equal to the number of reflecting elements (or multiple to it). In so doing, for the elevations close to 90° the even-paced integration with respect to ε was done, for the other elevations, such integration should be done with unequal step. The phase in the aperture of the main mirror Φ^0 is computed by the formula $\Phi^0 = \Phi + \Delta\Phi$, where Φ is the phase with an ideal surface of the main mirror, $\Delta\Phi$ is the addition to the phase when errors in the settings of the panels of the main mirror are present.

The phase Φ was computed by the formulae presented in the paper by Majorova (2002); for the calculation of $\Delta\Phi(\varepsilon, y)$ we used the formula:

$$\begin{aligned}\Delta\Phi(\varepsilon, y) &= 2\pi/\lambda\,[\Delta r(\varepsilon)\cos^2(H/2) \\ &+ (y - b/2)tg(\Delta u(\varepsilon))],\end{aligned}$$

where Δr is the error in setting the Nth panel in radius, Δu is the error in setting the Nth panel in elevation, N is the number of the panel, y is the coordinate in the vertical aperture of the panel, b is the height of the panel. For the elevations $H \simeq 90°$ the relationship $\varepsilon = 0.4°(N - 600)$ is satisfied. The error of setting the panels in azimuth was not taken into account since the BP of the panel is by almost two orders of magnitude wider than the BP of the radio telescope.

In Fig. 24(a) are displayed the drift scans of the point source 3C 84 at $\lambda 7.6$ cm wavelength across the horizontal cross-section $\Delta H = \pm 20'$ in the 2001 October observations, and the computed curves of the same cross-sections of the BP without including the errors in setting the panels of the main mirror. Fig. 24(b) shows the computed curves of the same cross-sections but with including the errors of setting the panels in the coordinate of elevation. As the latter we

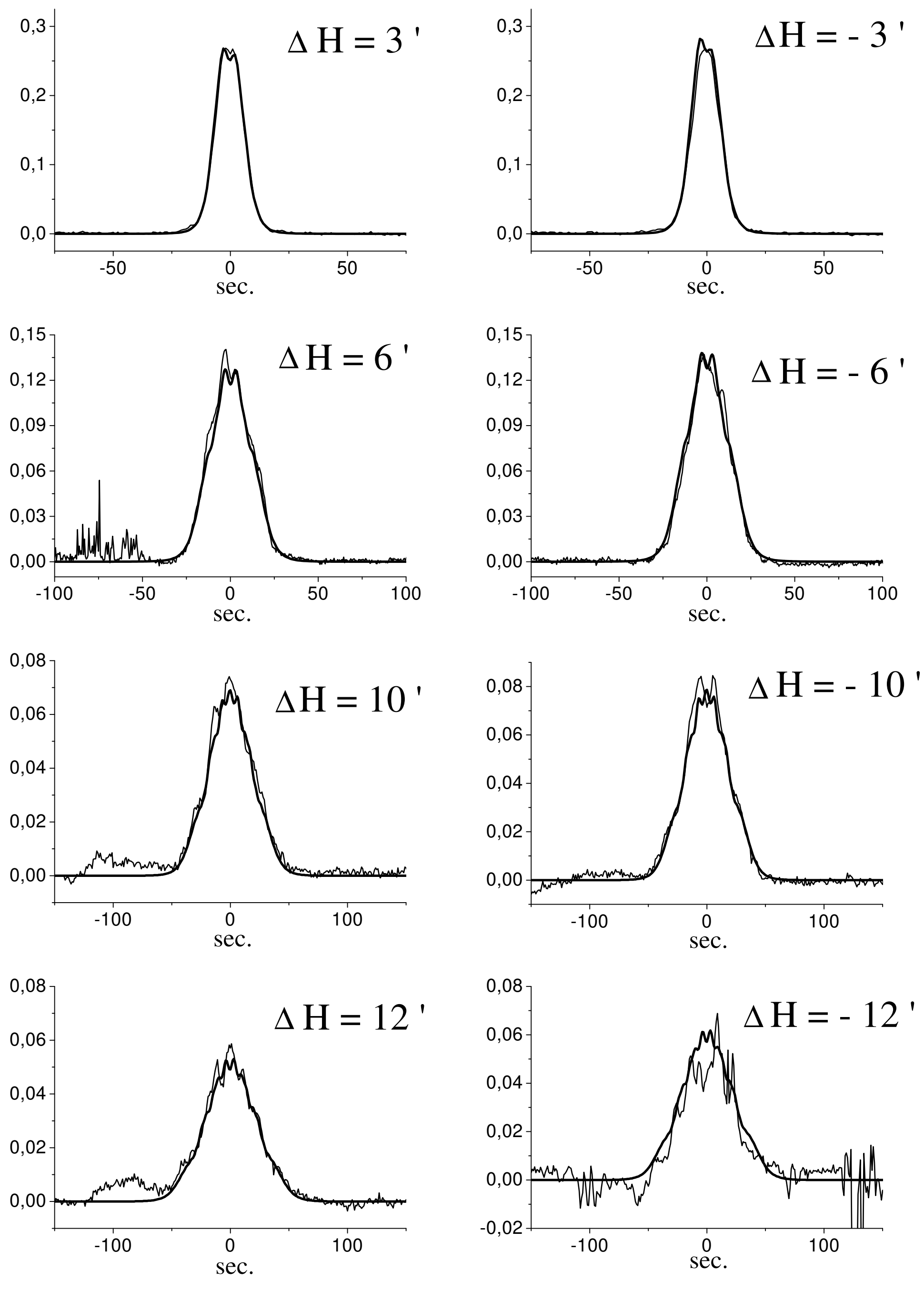

Figure 21: *The drift scans of the point source 3C 84 (0316+41) at the wavelength λ7.6 cm across the horizontal cross-section of the BP (thin lines) and the computed horizontal cross-sections of the BP corresponding to them (bold lines). The observations were carried out in April, 2002. The shift of the horn is $\Delta = 2.9\lambda$.*

used the differences between the new and old kinematic corrections in the elevation, which were measured by S.Golosova's geodesic group and were kindly given by them for the calculations, and also the errors in the position of the panels, which are registered by the ACS in an actual observation (the so-called "failures" of the panels). Since the measurements of kinematic corrections had not yet been completed by the moment of calculations, we had information only about 50 panels. The number of the panels in which the kinematic corrections changed by more than $10'$ turned out too small, the change in the kinematic corrections in elevation was mainly not larger than $\pm 2'$. Provision for these elevation errors in setting the panels caused a change in the structure of the computed curves (Fig. 24(b)). However, in order to

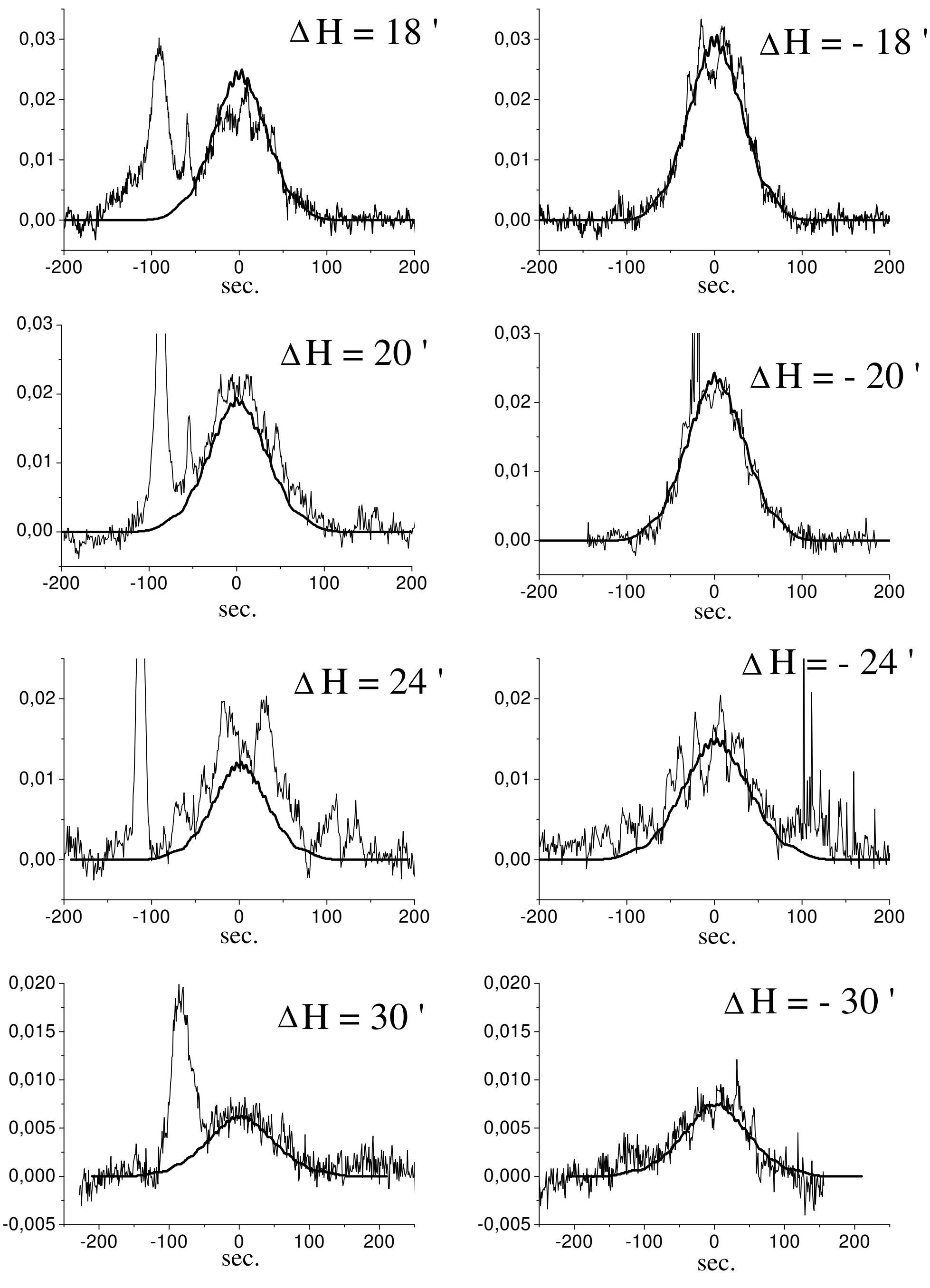

Figure 22: *The drift scans of the point source 3C84 (0316+41) at the wavelength* $\lambda 7.6$ *cm across the horizontal cross-section of the BP (thin lines) and the computed horizontal cross-sections of the BP corresponding to them (bold lines). The observations were carried out in April, 2002. The shift of the horn is* $\Delta = 2.9\lambda$.

bring the computed and experimental curves to correspondence, a systematic elevation error $\Delta u = 1.7'$ (4 precise graduation marks in elevation) had to be specified. One precise graduation mark of the synchro in elevation is $25''$, one precise graduation mark of the synchro in radius equals 0.17 mm.

For calculations of BPs in different horizontal cross-sections we also involved the data on the change of "zero" positions of the panels obtained from the results of auto-collimation adjustments of the antenna. The differences of the "zero" positions of the panels between two sequential auto-collimation adjustments, one of which was done before the observing run, the other after that, have been used as the errors in radius Δr and elevation Δu. After the planned adjustment performed in 2002 March, for the calcula-

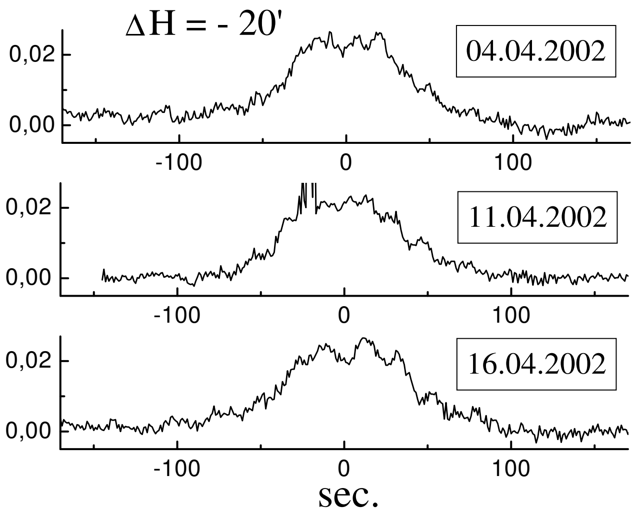

Figure 23: *The drift scans of the point source 3C84 (0316+41) at the wavelength λ7.6 cm across the horizontal cross-section of the BP $\Delta H = -20'$ on different days of observations.*

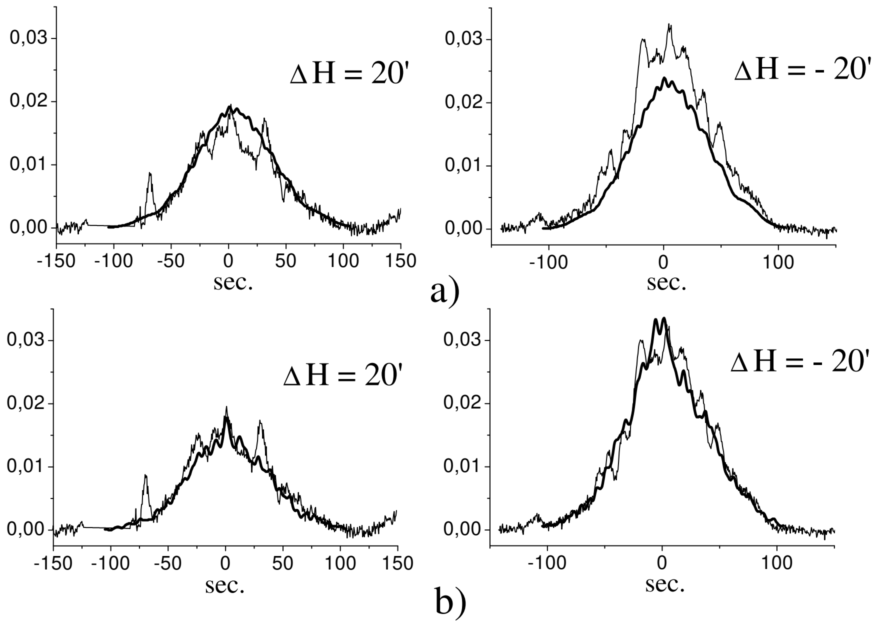

Figure 24: *The drift scans of the point source 3C84 (0316+41) at the wavelength λ7.6 cm across the horizontal cross-section of the BP (thin lines) and the computed horizontal cross-sections of the BP corresponding to them (bold lines). a) — calculation without provision for elevation errors in settings of the main mirror reflecting elements, b) — calculation with allowance made for errors in setting of the reflecting elements in elevations. Observing set of October 2001.*

tion of individual cross-sections of the BP the differences of the "zero" positions of the 2002 March and 2001 April adjustments were used. The bold lines in Fig. 25 show the computed cross-sections of the BP at λ7.6 cm and $H = 87.7°$ with allowance made for the elevation and radial errors, and the drift scans of the source 3C84 across the corresponding cross-sections of the BP (thin lines). Attention is attracted by the circumstance that the amplitude of the computed curves has approached the experimental ones without additional introduction of the systematic elevation error. The maxima of the BP increased in the cross-sections with negative ΔH, and decreased in the cross-sections with positive ΔH; the amplitude of the small-scale structure of the BP increased. Though in individual cross-sections a correlation in the structure of the computed and experimental curves was observed, we failed in getting their full coincidence. Apparently, the differences of the "zero" positions of consecutive adjustments do not give full information about the real position of the main antenna panels with respect to the perfect surface in an actual moment of observation of a given source. This manifests itself visually in the 2002 April observations.

At the beginning of the set the antenna was in a good state (less than a month after its adjustment), and at the end of the run more than 20 panels had significant errors in elevation (Fig. 28(a)). The state of the antenna degraded in rather a short time interval. As a result, the records of the BP cross-sections which were investigated at the beginning of the run ($\Delta H = \pm 10', \pm 20', \pm 30'$) were in a very good agreement with the calculated curves, but the records obtained at the end of the run ($\Delta H = -12', \pm 18', \pm 24'$) had a small-scale structure and differed markedly from the computed curves (Figs. 21, 22).

In a good state of the antenna the root-mean-square error of setting the panels in radius and elevation is not worse than 2–2.5 precise scale graduations of the synchro. Besides there are no panels with large elevation errors. Unfortunately, in actual observations such errors ("bounces") arise because of wear of the mechanisms for moving the panels. There also exist elevation errors in the position of the additional panels with respect to the surface of the main mirror panel. These additional panels are sheets two meters high which are made fast to the main surface panels at the top and bottom. The bold lines in Fig. 26 show the cross-sections of the BP computed with allowance for the occasional elevation errors in the setting of the additional panels with respect to the surface of the panel, the thin lines show the drift scans of the source 3C84 at $\lambda 7.6$ cm across the same cross-sections of the BP at the beginning of the 2002 April observations. The root-mean-square error of setting the additional panels with respect to the main surface of the panel is no less than $1' - 1.5'$.

Fig. 29(b) shows the cross-sections $\Delta H = \pm 20' \times \lambda[\mathrm{cm}]/7.6$ at the waves $\lambda 1.38$, 3.9, 7.6 and 31 cm calculated with allowance for elevation and radial errors, the mean square of which is 2.5 precise scale graduations of the synchro. As can be seen from the curves displayed in Figs. 26 and 29(b), the presence of small random errors in setting the panels in the elevation and radial coordinates and setting the additional panels in elevation does not cause significant distortion of the BP even in distant cross-sections. Fig. 29(a) presents for comparison the same cross-sections of the BP computed for a perfectly smooth surface of the main mirror at the wavelengths $\lambda 1.38$, 3.9, 7.6 and 31 cm for the source 3C84 ($H = 87.7°$). Random errors of the order of $\sim 2-3$ precise scale graduations of the synchro cause insignificant fluctuations of the BP in distant cross-sections; the value of these fluctuations even at the shortest wave (λ 1.38 cm) does not exceed a few per cent of the maximum BP (F_{max}) in this cross-section. At waves $\lambda \leq 7.6$ cm in the cross-sections $\Delta H = \pm 20'$ $F_{max} \simeq 0.02 \div 0.03 F_{max}(0)$. This is true when great bounces in the position of the panels in elevation are absent.

The picture changes dramatically if in the setting of the antenna for a given source there appear the panels with large errors in the coordinate of elevation. As can be seen from the curves shown in Figs. 27 and 29(c,d), the presence of such panels causes a considerable change in the structure of the BP in horizontal cross-sections. The thin lines in Fig. 27 are the drift scans of the source 3C84 across the immovable BP at the end of the 2002 April observations, the bold lines represent horizontal cross-sections of the BP $\Delta H = \pm 12', \pm 18', \pm 24'$ computed with provision for elevation and radial errors in the settings of the main mirror reflecting elements. As the latter, the differences of "zero" element positions in elevation and radius of two consecutive auto-collimation adjustments in March and June, 2002 (Fig. 28(a)) have been used. The data presented in Fig. 28 were kindly made available to us by the group of antenna adjustments and by the head of the LACSR G.V. Zhekanis. It is seen from Fig. 28(a) that at the moment of adjustment in 2002 June about 20 panels had large bounces of one sign in terms of elevation. That it is exactly them that cause distortions of the BP is shown by the comparison of experimental and computed curves. The computed curves get a distorted small-scale structure, the amplitude of the distortion increases with respect to F_{max} in a given cross-section as ΔH increases. That we cannot attain complete coincidence of the computed and experimental curves is explained by the fact that the differences of the "zero" positions used in computations give information about the state of the antenna only for the moment of the adjustment itself. Occasional damages of the mechanisms responsible for moving the panels in any of the coordinates or their replacement in the process of active use of the antenna between the adjustments lead to the fact that the values of "zero" positions of such a panel could be incorrect. Therefore the setting of a panel for a given source turns out to be in error. The damage of the mechanism of panels, which took place in April 2002, and also the influence of some other factors cause the appearance of panels with significant errors in elevations. The number of panels with erroneous "zero" positions and their distribution over the antenna changed during the observing set and there was no sufficient information to take into account these changes in calculations of the BP. In such cases adjustments of the antenna, not

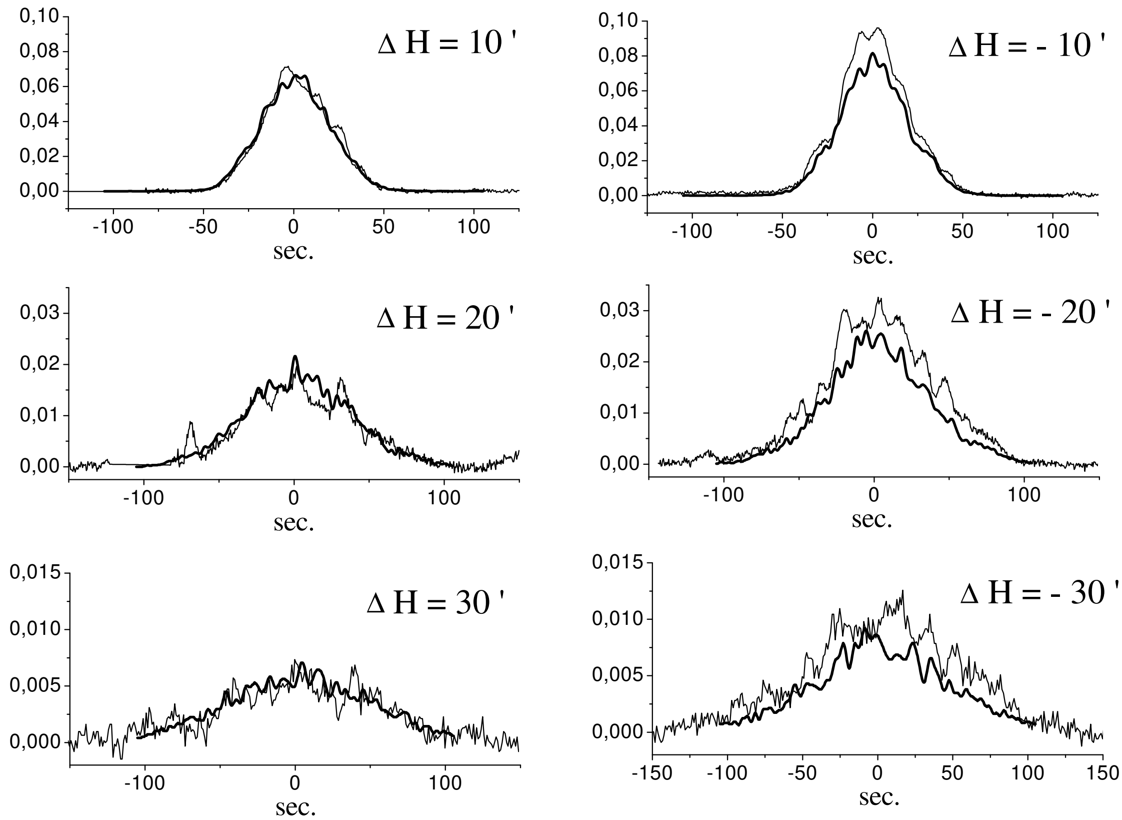

Figure 25: *The drift scans of the point source 3C84 (0316+41) at the wavelength λ7.6 cm across the horizontal cross-section of the BP in the 2001 October observations (thin lines) and the computed horizontal cross-sections of the BP corresponding to them with allowance for errors in settings of the main mirror reflecting elements in elevation and radius (bold lines). As the latter, the differences of "zero" positions in elevation and radius between auto-collimation adjustments in 2002 March and 2001 April were used.*

provided for by the plan, must be performed.

It is shown in Fig. 29 how the structure of horizontal cross-sections of the BP changes at different wavelengths with changing character of the distribution of elevation errors over the panels. The cross-sections in Fig. 29(a) are computed with "zero" position errors, the cross-sections in Fig. 29(b) are computed with elevation and radial errors, the mean square of which equals 2.5 precise scale graduations of the synchro, the cross-sections in Fig. 29(c) — with elevation errors corresponding to the difference of "zero" positions of the 2002 June and July adjustments (Fig. 28(b)), the cross-sections in Fig. 29(d) — with elevation errors corresponding to the difference of "zero" positions of the March and June 2002 adjustments (Fig. 28(a)). It can be well seen from these figures that a change in the number of panels with large elevation errors and their distribution over the aperture leads to a considerable change in the BP structure. These changes are the more pronounced the shorter is the wavelength. On condition that the number of panels with great errors is rather large, a general shift of the BP in elevation may occur if errors of one sign predominate. Note that radial errors also have an effect on the BP structure, but considerably weaker than bounces in positions of the panels in elevation.

Any errors in setting of the reflecting elements of the calculated position cause not only distortion of the BP structure but also a fall-down in gain of the antenna, i.e. a decrease in $F_{max}(0)$. The latter will be the more significant the shorter is the wavelength at which observations are performed.

The obtained results show that with the aid of the developed technique the BP of the radio telescope can be computed with sufficient accuracy, provided that reliable diagnostics of individual panels of the main mirror in all the coordinates is available. Partly such diagnostics is carried out in the automatic control system of the antenna. However, with convalescence and wear of the motion mechanisms this diagnostics turns out to be insufficient.

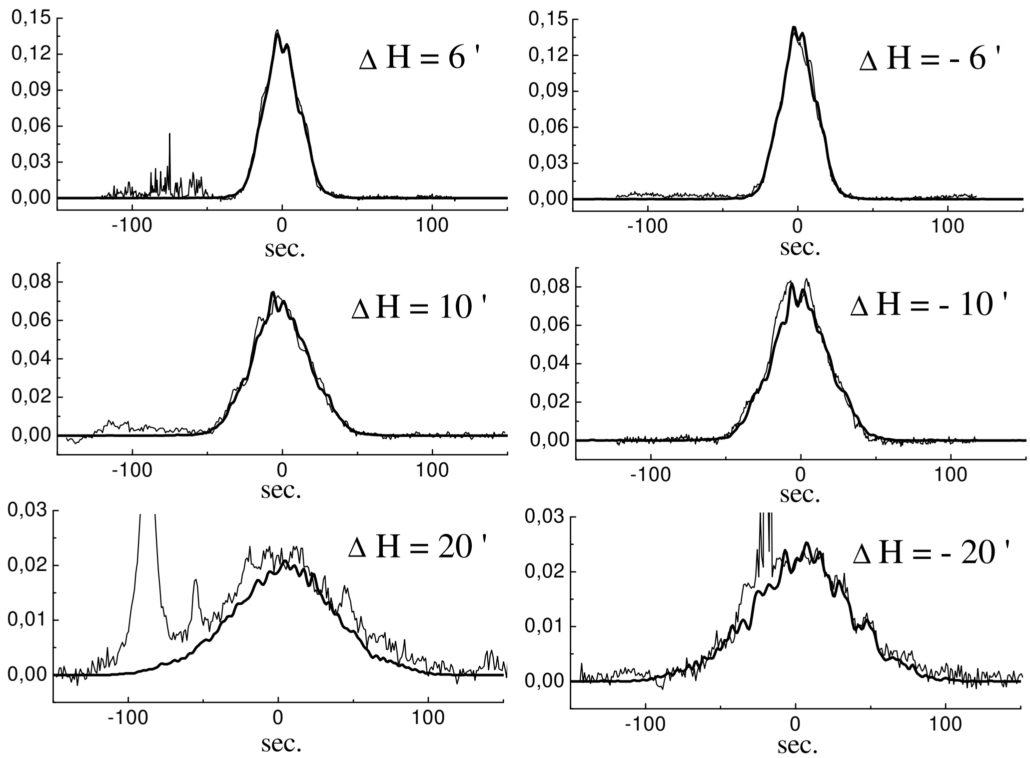

Figure 26: *The drift scans of the point source 3C 84 (0316+41) at the wavelength λ7.6 cm across the horizontal cross-section of the BP from the 2002 April observations (thin lines) and the computed horizontal cross-sections of the BP corresponding to them (bold lines). The calculation was performed with provision for occasional elevation errors in setting of the panels of the main mirror reflecting elements.*

5. Moon

Together with the investigations of the BP by point sources a modeling of transit of an extended source across the computed two-dimensional BP of RATAN-600 and a comparison of the results of modeling with actual records of transit of the Moon across the BP were made. The calculation of the two-dimensional BP was accomplished with the help of the program developed by Majorova (2002) under the assumption of perfectly smooth main mirror surface. Convolutions of the computed BP with the homogeneous disk of angular dimensions of the Moon at the waves λ1.38, 2.7, 3.9, 7.6, 13, 31, 47.6 cm were made. The elevations of the Moon, with the drift scans of which the comparison was made, proved to be 53.6°, and the phase of the Moon was 91.3°.

The background scattering brought by occasional errors of setting the panels was simulated at short wavelengths (λ1.38, 2.7, 3.9 cm). It was specified by the two-dimensional Gaussian, the halfwidths of which are equal in the horizontal and vertical planes (Baars, 1973) $\theta_x = 0.53\lambda/a$, $\theta_y = 0.53\lambda/c$, where $a = 2$ m is the width of the panel, c is the effective vertical size of the panel at short wavelengths.

The drift scans of the Moon were normalized to their maximum and compared with the normalized sum of convolutions $S = S_1 + pS_2$, where S_1 is the convolution of the BP with the homogeneous disk, S_2 is the convolution of the Gaussian of the scattered background with the homogeneous disk of the Moon. By way of selecting the coefficient p, the fitting of the computed and actual drift scans of the Moon across the BP at short wavelengths was made. The value of p being given, at which the discrepancy between the calculated and experimental curves is a minimum, with the aid of the technique stated in the paper by Gosachinsky et al. (1989) one can compute the root-mean-square error (σ) with which the panels of the main mirror at the moment of observations were set. The precision of the technique is about 5 %. The dotted line in Fig. 30 is the drift scans of the Moon at the wavelength λ1.38 cm, and the solid lines represent the computed curves at different values of the coef-

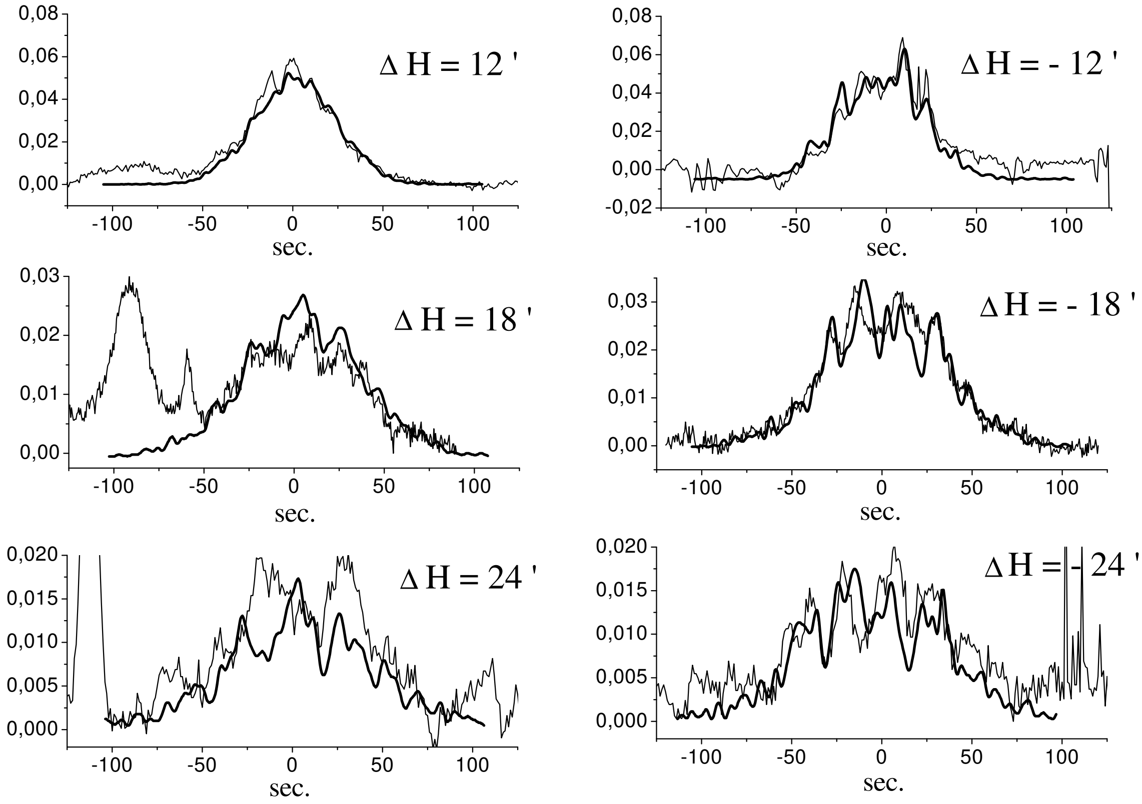

Figure 27: *The drift scans of the point source 3C84 (0316+41) at the wavelength λ7.6 cm across the horizontal cross-section of the BP in the 2002 April observations (thin lines) and the computed horizontal cross-sections of the BP corresponding to them with allowance for errors in settings of the main mirror reflecting elements in elevation and radius (bold lines). As the latter, the differences of "zero" element positions in elevation and radius of two consecutive auto-collimation adjustments in March and June, 2002 were used.*

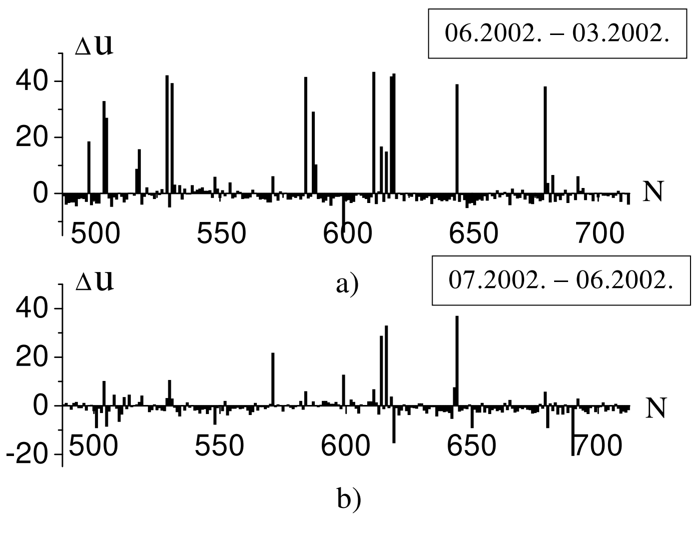

Figure 28: *The differences of the "zero" positions in the "elevation" coordinate of three sequential adjustments. Δu are given in precise scale graduations of the synchro. N is the number of the panel.*

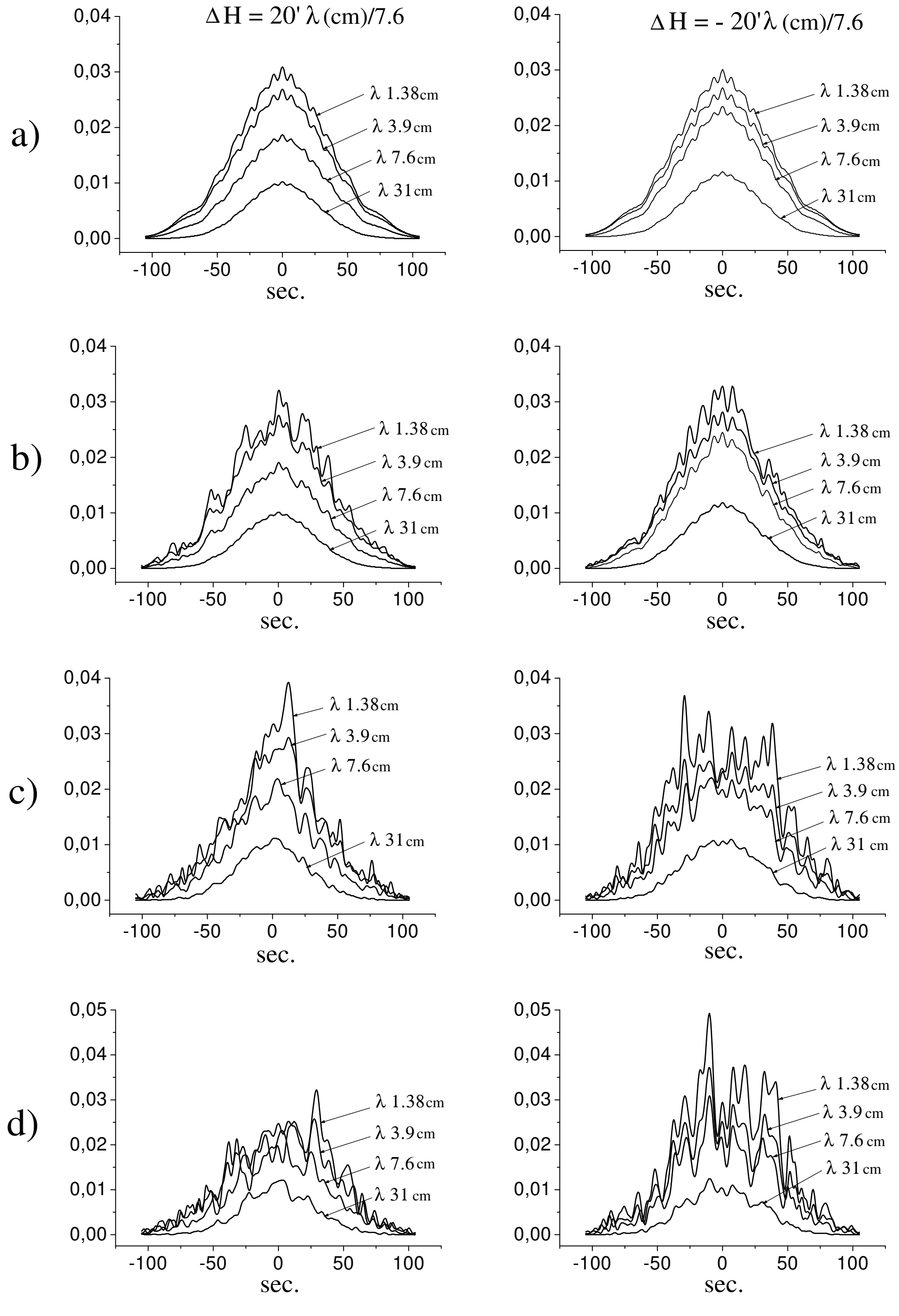

Figure 29: *The normalized horizontal cross-sections of the BP* $\Delta H = \pm 20' \times \lambda[\mathrm{cm}]/7.6$ *at different wavelengths computed for the main mirror surface: a) — without errors in settings of the panels, b) — with elevation and radial errors equal to 2.5 precise scale graduations of the synchro, c) — with elevation errors corresponding to the difference of the "zero" positions of the adjustments in 2002 June and July, d) — with elevation errors corresponding to the difference of the "zero" positions of the adjustments in 2002 March and June. The scale on the abscissa axis corresponds to the wave 7.6 cm. For other waves it should be multiplied by the coefficient* $\lambda[\mathrm{cm}]/7.6$ *(*$H = 87.7°$*).*

ficient p to which the values $\sigma = 0.8, 0.55, 0.31$ mm correspond. Fig. 31 displays the records of drift scans of Moon at the waves $\lambda 1.38$, 2.7, 3.9 cm (thin lines) and the computed curves corresponding to $\sigma = 0.55$ mm (bold lines).

Occasional errors do not affect the shape of the drift scan at wavelengths $\lambda \geq 7.6$ cm. At these wavelengths the experimental drift scans of the Moon

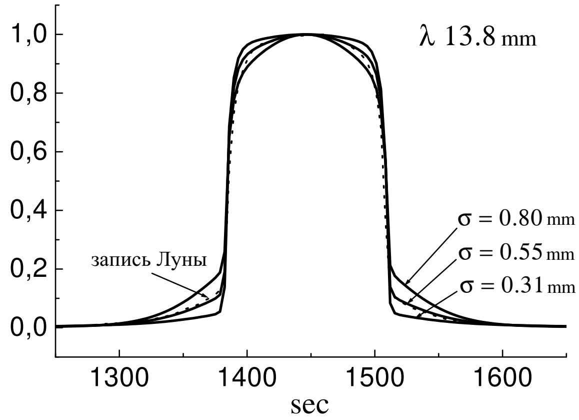

Figure 30: *The drift scans of the Moon at the wavelength* λ1.38 *cm (dotted line) and the computed curves corresponding to the values of errors in radius* $\sigma = 0.8$, 0.55, 0.31 *mm (solid lines).*

and the convolutions of the two-dimensional BP were compared with the disk of homogeneous brightness of the Moon's angular dimensions. The drift scans and convolutions were normalized to their maximum. In Fig. 31 they are shown by thin and bold lines, respectively. In all the records, but for those with dominating receiver's noises, the experimental and calculated curves are almost identical.

6. Aberration curves

During the observations in October, 2001 relations between the maximum values of the BP in the central cross-section F_{max} and the transverse displacement Δ of the receiving horn from the antenna focus (the so called aberration curves) were measured using the reference sources PKS 1921-36 ($H = 17°$), PKS2230+10 ($H = 57°$), 3C48 (0134+32) ($H = 79°$) and 2200+42 (Bl Lac) ($H = 88°$). They are shown by squares in Fig. 32. In the same figure the solid lines represent the aberration curves computed with the aid of the refined calculation of the BP, the dotted lines are the aberration curves computed by the program of Korzhavin (1979). It can be seen that at elevations $\leq 80°$ the curves computed by these programs only slightly differ and are in good agreement with the results of measurements. For the elevations close to 90° there are considerable discrepancies in the behavior of the computed curves. As it was shown in the paper by Majorova (2002), provision for the diffraction effects and the finite width of the ring of the main mirror caused a significant narrowing of the aberration-free zone near the zenith. The experimental data obtained from aberrations with large displacements of the horn from the focus yield an ambiguous result. The values of F_{max} corresponding to negative Δ lie below the computed curves, while those corresponding to positive Δ are somewhat above them. Such asymmetry may be interpreted as non-symmetry in installation of the horns at the wavelength 1.38 cm on the focal line of the secondary mirror, along which the receiving horns are located. Probably, additional measurements are needed to refine the results obtained. Note, that at high elevation with large transversal displacements of the receiving horn from the focus the source passes somewhat below the central cross-section of the BP, which should be taken into account when computing the aberration curve.

7. Conclusions

The observations of reference point sources conducted in three runs of observations in 2001–2002 made it possible to investigate in details the BP of RATAN-600 in a wide range of elevations and wavelengths with the focused antenna and in the presence of aberrations. Relationships were derived between the maximum BP values in the horizontal cross-sections and the value of the shift of the cross-section with respect to the central one in elevation, $F_{max}(\Delta H)$. Comparisons of drift scans of point sources across different horizontal cross-sections of the BP with the corresponding computed cross-sections were made. Two-dimensional BPs of RATAN-600 were constructed from individual observed cross-sections.

A comparison of the relations $F_{max}(\Delta H)$ and the drift scans of the source across the horizontal cross-sections of the BP with the computed curves showed good agreement of the experimental data with the results of calculations by the program, in which the diffraction effects in the Fresnel zone and the finite width of the main mirror were taken into account. Under a good state of the antenna, the coincidence of the experimental and computed curves is reached

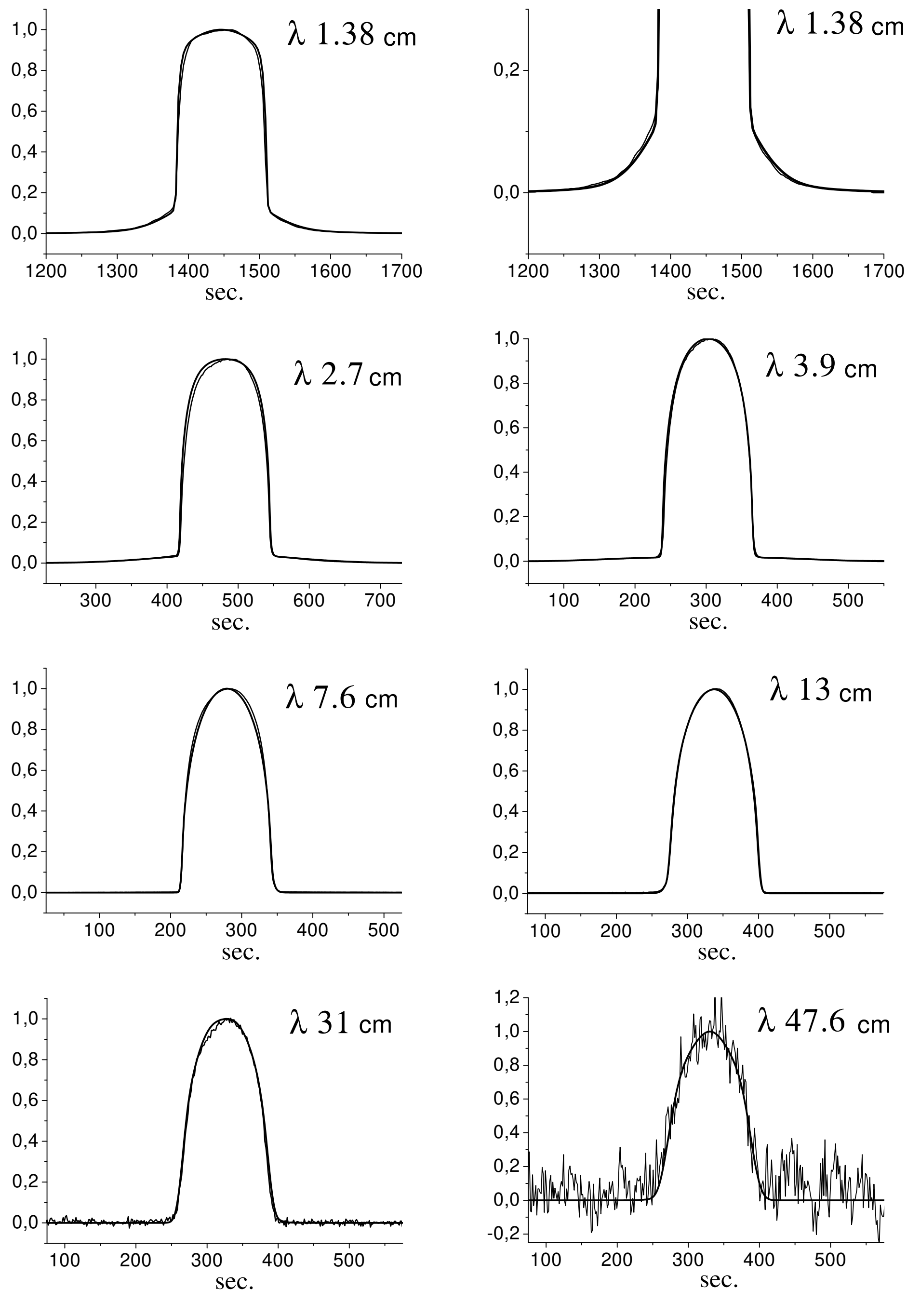

Figure 31: *The drift scans of the Moon across the BP of RATAN-600 at the waves* $\lambda 1.38 - 47.6$ *cm (thin lines) and the convolutions of the two-dimensional calculated BP with the uniform disk of the sizes of the Moon (bold lines).*

at the level 0.005 of the BP maximum in the central cross-section. With appearance of serious errors in setting the reflecting elements of the main mirror in elevation, the structure of the BP at distant cross-sections may change significantly both in the shape and amplitude. Individual cross-sections of the BP were simulated in the presence of errors in setting the panels in elevation and radial coordinates and errors in setting the additional panels on the elements of the antenna. It is shown how the structure of the BP changes at distant cross-sections with changes of the value and character of distribution of these errors over the aperture of the main mirror. Allowance made for such errors is important in observations at short wavelengths because, besides the change in the structure of the BP, such errors may cause a considerable

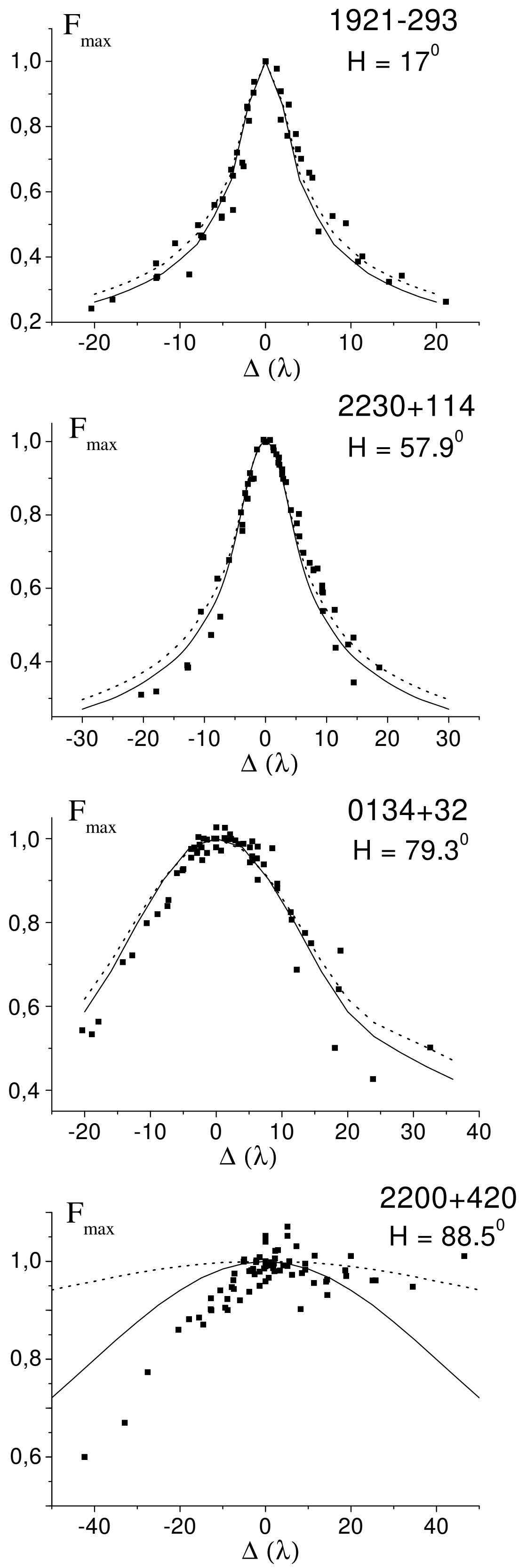

Figure 32: *The aberration curves $F_{max}(\Delta)$ derived from observations of reference sources (squares) computed with the aid of the refined calculation of the BP (solid lines) and those calculated by the program of Korzhavin (dotted line).*

fall-down of the antenna gain. It is also important in the processing of data of deep surveys and "cleaning" of records from bright "off-axis" background sources passing across distant cross-sections of the BP.

A comparison was made of the experimental drift scans of the Moon and convolutions of the computed two-dimensional BP with the uniform disk of the Moon in the whole working wavelength range of RATAN-600. The computed and experimental curves showed a good fit. At short wavelengths ($\lambda \leq 3.9$ cm) for fitting of the experimental and computed curves we used the technique proposed in the paper by Gosachinsky et al. (1989) with the aid of which the root-mean-square error of setting the reflecting elements of the main mirror in radius can be determined. This error was equal to 0.55 mm.

By means of observations of point cosmic sources, measurements of aberration curves of the radio telescope at different elevations were made. The curves had a good fit to the computed aberration curves but for the elevation $H = 88°$. The discrepancy in plotting the computed and experimental curves with very large displacements of the horn from the focus is likely to be associated with incorrect setting of the horns at the wavelength 1.38 cm along the focal line of the secondary mirror.

The measurements of the BP made it possible to check the accuracy of calculation and reveal important effects which influence the behavior of the BP and its stability in time. These effects are connected with the precision of setting the main mirror reflecting elements and may also be taken into account in the computations provided that diagnostics of the state of the antenna is reliable.

Acknowledgements. The authors thank S.Ya. Golosova, I.V. Berlizev, G.V. Zhekanis for the data on the state of the antenna, N.N. Bursov for help in observations and Yu.N. Parijskij for valuable remarks and discussion of the paper.

References

Gosachinskij I.V., Majorova E.K., Parijskij Yu.N., 1989, Soobshch. Spets. Astrofiz. Obs., **63**, 38

Esepkina N.A., Bakhvalov N.S., Vasil'ev B.A., Vasil'eva L.G., Temirova A.V., 1979, Astrofiz. Issled. (Izv. SAO), **11**, 182

Korzhavin A.N., 1979, Astrofiz. Issled. (Izv. SAO), **11**, 170

Kuz'min A.D., Solomonovich A.E., 1964, Radioastronomical techniques of the antenna parameters, Sov. Radio

Temirova A.V., 1983, Astrofiz. Issled. (Izv. SAO), **17**, 131

Temirova A.V., 1985, Astrofiz. Issled. (Izv. SAO), **19**, 101

Baars J.W.M., 1973, IEEE Trans. Antennas and Prop., **AP-21**, 461

Majorova E.K., 2002, Bull. Spec. Astrophys. Obs., **53**, 132